URBAN MINING OF RARE EARTH ELEMENTS FROM RARE EARTH MAGNETS – ALTERNATE SOLVENTS FOR EXTRACTION

ENCH4LA

LABORATORYY/INDUSTRY PROJECT

2021

Student Name: Sohana Bridgemohan

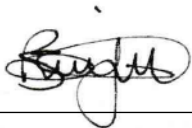Student Number: 218010264

Partner's Name: Riyantha Moodley

Partner's Student Number: 218009136

Supervisors: Prof. P. Naidoo, Dr M. Williams-Wynn, Dr K. Moodley

Statement of Authorship

I, Sohana Bridgemohan, declare that:

(i)   The information reported in this report, except where otherwise indicated, is my original work.
(ii) This report has not been submitted for any degree or examination at any other university.
(iii) This report does not contain other persons' data, pictures, graphs or other information, unless specifically acknowledged as being sourced from other persons.
(iv) This report does not contain other persons' writing, unless specifically acknowledged as being sourced from other researchers. Where other written sources have been quoted, then:
   a. Their words have been re-written but the general information attributed to them has been referenced;
   b. Where their exact words have been used, their writing has been placed inside quotation marks, and referenced.
(v)   This report does not contain text, graphics or tables copied and pasted from the internet, unless specifically acknowledged, and the source being detailed in the thesis and in the references sections.

_____   08/06/2021

STUDENT'S SIGNATURE   DATE

Acknowledgements

The following are thanked for their contributions to the work produced in this report:

Abstract

The recovery of rare earth elements through hydrometallurgical methods from waste electronic equipment, such as neodymium contained in neodymium-iron-boron (NdFeB) magnets, seeks to provide an alternative supply to meet the growing demand of these critical materials. Solvent extraction is the process of interest, wherein metal extraction data is required to accelerate the development of these commercial processes. Thus, the aim of this research project was to investigate the degree of extraction of iron from an aqueous nitric acid solution of varying concentration (0.1M, 0.5M and 0.9M), using bis-(2-ethylhexyl) phosphate (0.5M) dissolved in n-dodecane. An existing bench-scale liquid-liquid extraction (LLE) apparatus was used to perform duplicate measurements at ambient conditions. The post-extraction concentrations were determined via ICP-OES analysis. The experimental method was successfully verified through a neodymium test system at 25.2°C and 100.09kPa. The distribution was inversely proportional to the nitric acid concentration, which is consistent with that reported in literature. The highest neodymium distribution, 10.674, was observed at the lowest, 0.1M, feed nitric acid concentration. The distribution of iron in the aforementioned acid concentrations and solvent mixture, at 24.55°C and 100.305kPa, was found to be unaffected by variations in the nitric acid concentration. The distribution ratio remained fairly constant at approximately 20. Ionic liquids have the potential to improve the extent and selectivity of metal extraction. Hence, the effect of doping the organic phase with 0.1M of ionic liquid, tributylmethylphosphonium methyl sulfate, on the extraction of iron was investigated. Due to phase splitting in the organic phase, this experiment was not pursued further. The extraction selectivity of the aforementioned liquid-liquid system was investigated in a combined metal oxide system of neodymium and iron, at 21.45°C and 99.605kPa. The highest neodymium extraction selectivity was observed at the lowest nitric acid concentration (0.1M), wherein a distribution and separation factor of 926.947 and 65.633 were observed, respectively. Overall, excellent reproducibility in the duplicate measurements was observed. Based on the results, the feasibility of this separation method within a commercial scale recycling process was inferred. Recommendations for investigating phase splitting and ionic liquid doping on the distribution of iron, as well as methods to improve the ICP calibration, were provided.

Table of Contents

Table of Figures

Table of Tables

1 Introduction

Rare earth elements (REEs) refer to all lanthanide elements, as well as scandium and yttrium (Balaram, 2019). REEs are crucial components in a number of existing and developing modern technologies, due to their favourable physical and chemical properties; their main applications being catalyst and rare earth magnet production (Balaram, 2019; Haque, et al., 2014). In particular, neodymium-iron-boron (NdFeB) permanent magnets are of interest in this project. These magnets, among other REEs, are especially important in renewable energy technology and electric vehicles - these being its largest end-use applications (Goodenough, et al., 2018). This has led to a steep rise in the demand of NdFeB magnets that is expected to grow with the shift towards 'green' economies, as seen in Figure 1-1 (Gregoric, et al., 2018; Roskill, 2016).
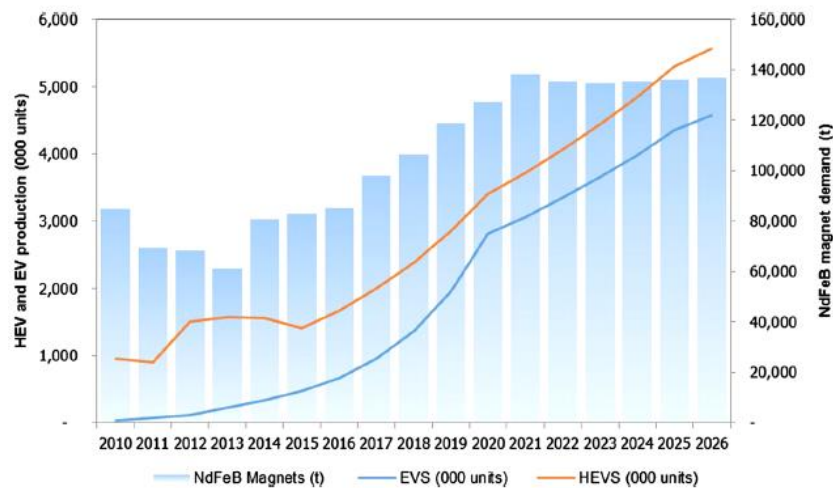
Figure 1-1: Projected production of hybrid electric vehicles (HEVs) and fully electric vehicles (EVs) versus NdFeB magnet demand (Roskill, 2016)

REEs typically occur in low concentrations within natural deposits, thus limiting economical mining operations (Wang, et al., 2017). Additionally, run-of-mine processing requires concentrated chemical acids which pose environmental hazards (Gregoric, et al., 2018). REEs have been classified as 'critical' materials due to their technological importance and the uncertainty in their supply chain as a result of quotas imposed by China – the largest REE producer (Massari & Ruberti, 2012). Furthermore, REEs currently have poor substitution potential with other cost effective materials, thus a sustainable supply of REEs is required to meet the growing demand of its end-use technologies (Dent, 2012).

Collectively, these factors of supply and demand have encouraged the development of REE extraction processes from secondary sources, such as recycling through urban mining. Waste electrical and electronic equipment (WEEE) recovered or diverted from landfills contain these materials in higher purities than in natural ores and are a viable recycling source (Wang, et al., 2017). Some examples of WEEE include mobile phones, LCD screens, with computer hard drives and loudspeakers being typical waste sources of NdFeB magnets.

Hydrometallurgical, pyrometallurgical and gas-phase extraction are the main existing rare earth magnet recovery routes available. Hydrometallurgical processing is considered the most advantageous recovery method and is thus the method considered in this study (Binnemans, et al., 2013). This process involves crushing and leaching of the waste material into a leachate solution. The aqueous solution is then contacted with an organic extractant to selectively remove the desired rare earth ions during solvent extraction, to be further processed thereafter.

The solvent extraction step is of interest in this investigation. Liquid-liquid equilibrium (LLE) data for neodymium, iron and boron systems are required to support the development of commercial NdFeB recycling processes. The extraction data of the individual components is necessary to enable future studies into the extraction behaviour from a real leachate solution containing all three elements. There is currently a limited collection of published neodymium extraction data, though there is scarce iron and boron data published in conjunction. Additionally, the growing number of available solvents, extractants and diluents result in many possible liquid-liquid system combinations, from which LLE measurements can be obtained. Bis-(2-ethylhexyl) phosphate (HDEHP) is one of the most efficient organophospohorous extractants, and is used in this study (Hidayah & Abadin, 2018)

Furthermore, the development of ionic liquids (ILs) motivates its incorporation into LLE measurements. ILs are molten salts with melting points below 100°C, with unique properties such as low volatility and high thermal stability, among others (Binnemans, 2007; Sun, et al., 2012). Ionic liquids also pose a sustainable alternative to the typical volatile organic compounds (VOCs) used as diluents in the solvent extraction process, further encouraging its use (Qi, 2018). One such class of IL, phosphonium-based ionic liquids, has been increasingly used in LLE applications, with the potential to improve the selectivity of REE separation (Ferreira, et al., 2012; Sun, et al., 2012).

The aim of this research project is to investigate the degree of extraction of iron from an aqueous nitric acid solution, using HDEHP dissolved in n-dodecane. The measurements are to be performed using an existing bench-scale LLE setup. This aim will be met through the execution of the following objectives:

Careful of tense

i. Verifying the experimental method using a neodymium(III) oxide test system.
ii. Measurement of the distribution ratio of iron with varying nitric acid concentrations at 25°C, to establish the optimal aqueous acid concentration for recovery.
iii. Measurement of the distribution ratio of iron with varying nitric acid concentrations at 25°C, with the organic extractant phase doped with an ionic liquid, tributylmethylphosphonium methyl sulfate ($[(C_4)_3PC_1][MeSO_4]$).
iv. Measurement of the distribution ratios of iron and neodymium from a combined metal oxide system, with varying nitric acid concentrations at 25°C to establish the selectivity of the liquid-liquid system.
v. Inferring the feasibility of this separation method as a pilot- or commercial-scale process.

This research project was performed in conjunction with an investigation into the extraction of neodymium by Mr Thulani Bayeni, as a post-graduate study at the University of KwaZulu-Natal. The measurements from this project complements the MSc Eng. study as it involves generating the extraction data of one of the remaining constituent elements in NdFeB magnets, iron, using the same liquid-liquid system and apparatus. It is understood that no data has been published for the extraction of either of these elements using this liquid-liquid system, and is the motivation for conducting these measurements.

Conditions of 25°C and atmospheric pressure were selected to obtain reference measurements to assess the system behaviour at ambient conditions. This would correspond to the cheapest and simplest operation for a scaled-up process of this system. Future work may perform measurements at elevated temperatures to assess the change in system performance with reference to the ambient conditions presented in this work.

A phosphonium based ionic liquid was selected to investigate its effect on the distribution measurements due to its aforementioned potential to improve the extent and selectivity of separation reported in literature. Of the reported IL-systems investigated in literature, the organic diluent was completely replaced by the IL of interest. However, the effect of small quantities of IL is investigated instead, due to the high cost of these materials. Hence, these measurements will indicate the feasibility of a potentially more efficient process that is less capital intensive.

This report is presented in 7 chapters. Chapter 2 provides an overview of the relevant theoretical background to the system and analytical methods investigated in this study. Chapter 3 describes the materials, experimental method and equipment used, as per the post-graduate study conducted in parallel. Chapters 4 and 5 report the results and discussion thereof, respectively. Chapter 6 presents the conclusions made in this investigation, followed by recommendations for future work in Chapter 7.

2   Literature Review

This chapter begins with a brief description of existing REE recovery methods. A thorough explanation of the various aspects of LLE systems is presented: the types of aqueous solvents and organic extractants, component mechanisms and ionic liquids. Thereafter, details of the extraction equipment and analyses methods are reported.

2.1   Recovery Methods

In the context of end-of-life NdFeB magnets, there are three main REE recovery methods available: hydrometallurgical, pyrometallurgical and gas-phase extraction (Binnemans, et al., 2013). Pyrometallurgical processing allows for REEs to be obtained in their metallic form directly; however, it is highly energy intensive and produces large amounts of solid waste (Binnemans, et al., 2013; Prodius, et al., 2019). Gas-phase extraction transforms the metals into volatile chlorides, from which they are separated based on varying volatilities; though this requires large volumes of hazardous chlorine gas (Binnemans, et al., 2013). Hydrometallurgy, while requiring large volumes of chemical reagents, is much less energy intensive and results in less gaseous pollution. Additionally, hydrometallurgy can process a larger range of feed material of lower grades, while still producing high product purities (Tunsu, et al., 2015).

Hydrometallurgical processing is the broader recovery method of waste NdFeB magnets considered. In this context, hydrometallurgical processing involves pre-treatment of WEEEs through sorting and crushing to liberate sufficiently small sizes of feed material for enhanced separation and recovery (Wang, et al., 2017). During the subsequent leaching process, dissolution of the metal ions into an aqueous leaching solution occurs, from which ions are selectively removed during solvent extraction (Gregoric, et al., 2018).

2.2   Solvent Extraction

Solvent extraction is a separation process that utilises LLE, during which a solute is selectively transferred between two partially, or totally, immiscible phases. The carrier phase is contacted and vigorously mixed with an extractant in which the solute is more soluble, thus effecting separation through mass transfer (Seader, et al., 2011). Separation of different REEs is difficult due to their similar physical and chemical properties. Solvent extraction and ion exchange techniques are the current technologies used to accomplish these separations to produce single rare earth solutions or compounds (Xie, et al., 2014).

The aqueous carrier phase consists of mineral acid, such as hydrochloric (HCL), sulphuric (H_2SO_4) or nitric acid (HNO_3), in which NdFeB magnets easily dissolve (Peelman, et al., 2015). In this study, neodymium and iron each exist with a 3+ charge in the aqueous HNO_3 feed solution as cations. Each element is introduced to the aqueous carrier phase via dissolution of their corresponding oxides, namely neodymium (III) oxide, and iron (III) oxide, and dissociate according to Equations 2-1 and 2-2 respectively:

$$Nd_2O_3 + 6H^+ \rightleftharpoons 2Nd^{3+} + 3H_2O \qquad (2\text{-}1)$$

$$Fe_2O_3 + 6H^+ \rightleftharpoons 2Fe^{3+} + 3H_2O \qquad (2\text{-}2)$$
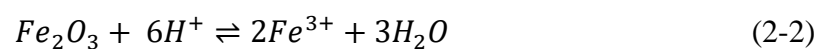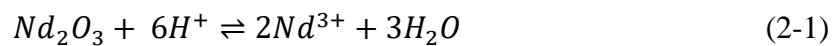
The organic phase consists of an extractant that transfers the dissolved solute out of the aqueous phase (Gregoric, et al., 2017). The separation efficiency, selectivity and thus extent of separation, is dependent on the extractant chosen. The ideal extractant is cost effective while having a high metal selectivity. Additionally, the extractant should be sufficiently insoluble in the aqueous phase to ensure aqueous phase stability (Hidayah & Abadin, 2018).

2.2.1   Organic Extractants

Xie, et al. (2014) summarised the different types of extractants into three main categories: cation exchangers, anion exchangers and solvation extractants. Solvation exchangers extract metal ions from the aqueous phase as they form complexes with counter ions. However, these extractants have lower distribution coefficients due to water molecules occupying remaining coordination sites on those complexes (Tunsu, et al., 2019). Anion exchangers remove metal ions from the aqueous phase in the form of anionic complexes, thus are only effective in strong ionic solvents in the extraction phase (Hidayah & Abadin, 2018).

Cation exchangers are known to have a higher separation efficiency than the other types of extractants. The separation achieved with cation exchangers is favoured by increasing the pH or reducing the acidity, of the aqueous phase - thus are alternatively called 'acidic extractants'. The stripping process used to harvest the extracted ions from the organic phase requires an aqueous stripping agent and is favoured by highly acidic stripping agents (Hidayah & Abadin, 2018; Xie, et al., 2014). According to Qi (2018), the mechanism for these extractants comprises of five equilibrium processes and have been described as follows (Qi, 2018):

 i. Solution equilibrium distribution of the extractant between both phases.
 ii. Dissociation of the extractant in the aqueous phase (formation of extractant anions).
 iii. Dissociation of the rare earth compound (into rare earth ions) in the aqueous phase.
 iv. Complex formation in the aqueous phase: rare earth ions with the extractant anions.
 v. Dissolution of the complex from the aqueous phase into the organic phase.

The extraction mechanism for trivalent REEs and cationic exchangers is summarised by Equation 2-3. Alternatively, Equation 2-4 is applicable when the extractant exist as a dimer; in this case, the rare earth complex that forms contains undissociated organic acid (Xie, et al., 2014; Gregoric, et al., 2017).

$$Ln^{3+} + 3\overline{HA} \rightleftharpoons \overline{LnA_3} + 3H^+ \qquad (2\text{-}3)$$

$$Ln^{3+} + 3\overline{H_2A_2} \rightleftharpoons \overline{Ln(HA_2)_3} + 3H^+ \qquad (2\text{-}4)$$
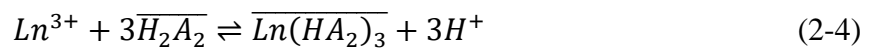
where, Ln refers to the rare earth and A refers to the organic anion, H_2A_2 refers to the dimeric form of the organic acid and the overbar denotes species in the organic phase.

Typically, the extractant is dissolved in an organic diluent to reduce the organic phase viscosity and facilitate extraction (Gregoric, et al., 2017). The polarity and hydrogen bonding affinity of the diluent improves the hydrophobicity of the extractant complexes and thus improves the extraction efficiency (Gregoric, et al., 2017). The ideal diluent has a low aqueous phase solubility, volatility and surface tension, while still being relatively inexpensive and accessible (Batchu & Binnemans, 2018). n-Dodecane, a non-polar, straight-chained hydrocarbon is used as the organic diluent in this study.

2.2.2 Bis-(2-ethylhexyl) phosphate (HDEHP)

Bis-(2-ethylhexyl) phosphate (HDEHP), also referred to as di-(2-ethylhexyl) phosphoric acid (D2EHPA), is the cationic extractant used in this study. It is one of the most efficient organophospohorous acids commonly used in the extraction of REEs (Hidayah & Abadin, 2018). The central phosphorous atom is attached via double bonds to an oxygen atom. The hydrogen atoms from two out of three hydroxyl groups are substituted with 2-ethylhexyl organic chains to form HDEHP, shown in Figure 2-1 (Nayak, et al., 2014). Pure HDEHP exists as a stable dimer with hydrogen bonds in non-polar diluents, as shown in Figure 2-2 (Qi, 2018).
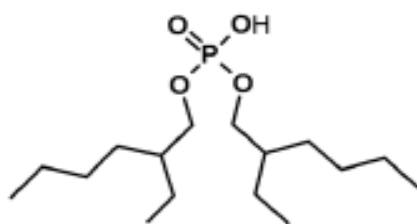
Figure 2-1: Structural formula of bis-(2-ethylhexyl) phosphate (Nayak, et al., 2014)
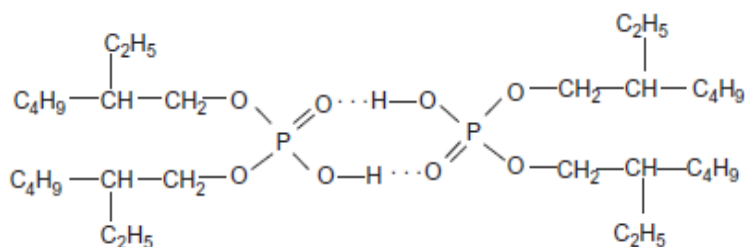
Figure 2-2: Dimeric form of bis-(2-ethylhexyl) phosphate (Qi, 2018)

Nayak, et al. (2014) performed LLE experiments for the extraction of americium from an aqueous nitric acid solution of varying concentrations (0.1M – 4M HNO_3) using 0.25M HDEHP in n-dodecane. The authors showed that for every Am^{3+} transferred into the organic phase, three H^+ ions were equivalently released into the aqueous phase, with a reported slope of -3 in Figure 2-3. A similar behaviour was reported for the extraction of europium (Nayak, et al., 2014). The authors also conducted measurements using the TODGA extractant, which forms stable metal complexes and has a relatively high affinity for REEs (Nayak, et al., 2014). Additionally, a combined TODGA and HDEHP organic phase was used to explore the synergistic extraction mechanism exhibited by combined solvents (Xie, et al., 2014). However, TODGA has not been considered in this investigation due to its associated cost.
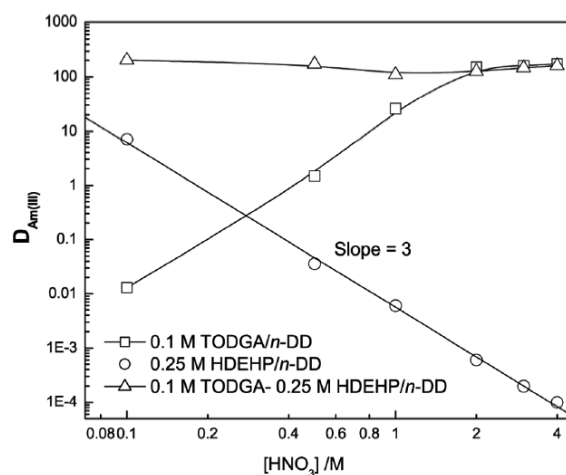
Figure 2-3: Distribution ratio of Am(III) as a function of nitric acid concentration (Nayak, et al., 2014)

This result experimentally verifies the extraction mechanism described in Equation 2-4 for the dimeric form of HDEHP, as reported by Gregoric, et al. (2017) and Xie, et al. (2014). Thus, for the same LLE system of interest in this study, the mechanism is expected to be consistent, according to Equation 2-5 and 2-6, where $Fe(HA_2)_3$ and $Nd(HA_2)_3$ are the resulting complexes soluble in the organic phase (Gregoric, et al., 2017). These Equations indicate that for every ion of neodymium or iron extracted into the organic phase, three hydrogen cations are released. Hence, three hydronium ions are expected to form in the aqueous phase. Thus an increase in the aqueous acid concentration is expected to occur during extraction.

$$Nd^{3+} + 3\overline{H_2A_2} \rightleftharpoons \overline{Nd(HA_2)_3} + 3H^{3+} \qquad (2\text{-}5)$$

$$Fe^{3+} + 3\overline{H_2A_2} \rightleftharpoons \overline{Fe(HA_2)_3} + 3H^{3+} \qquad (2\text{-}6)$$
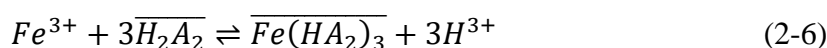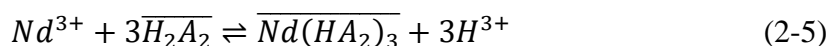
The HDEHP dimeric structure does not break during extraction, rather, one of the POO^- groups participates in the extraction. The dimer only separates if the metal ion loading in the organic phase is beyond a certain concentration. This results in the formation of an undesirable gel-like liquid phase, containing precipitated metal-extractant complexes, leaving behind a lighter, diluent rich-layer in the organic phase (Qi, 2018; Rout, et al., 2011). The limiting organic concentration (LOC) of HDEHP is expressed as a ratio of equilibrium concentrations: $[Ln^{3+}]$: [HDEHP] = 1: 6 (Qi, 2018). A chemical modifier may be added to the organic phase to prevent the formation of this third phase, such as tri-n-butyl phosphate (TBP). Alternatively, the aqueous acid concentration may be increased. (Gregoric, et al., 2017; Qi, 2018).

2.2.3   Ionic Liquids

Ionic liquids (ILs) are molten salts with melting points below 100°C (Binnemans, 2007). ILs are considered environmentally friendly alternatives to traditional volatile organic diluents; with qualities such as low volatility and thermal stability. Additionally, these chemicals have shown a great improvement in the extent, and the selectivity, of separation in the literature (Sun, et al., 2012). One such system is $[C_nMIM][NTf_2]$ (n=2, 4, 6, 8) in N-dodecyl aza-18-crown-6 extractant (Villemin & Didi, 2013). ILs are comprised of large organic cations and inorganic anions; thus, any desirable combination of these species may be selected. Hence, ILs are also "designer solvents" in this regard (Ferreira, et al., 2012).

Imidazolium-based ILs were the first ionic liquids used in metal extractions, for which most IL extraction data is published (Villemin & Didi, 2013). Phosphonium-based ionic liquids (PBILs) contain a central phosphorous ion with four different bonding sites – thus a large variety of 'tailor-made' cations, and hence ILs, can be generated within this class (Ferreira, et al., 2012). Tributyl(methyl)phosphonium methyl sulfate ($[(C_4)_3PC_1][MeSO_4]$), shown in Figure 2-4, is used in this investigation. The hydrophobicity of ILs is enhanced by incorporating, and extending, alkyl chain substituents on the cation (Binnemans, 2007).
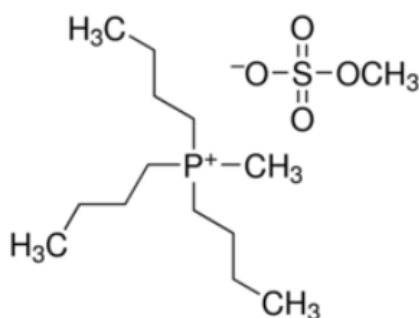
Figure 2-4: Chemical structure of tributyl(methyl)phosphonium methyl sulphate (Sigma-Aldrich , n.d.)

The improved extent and selectivity of separation, as well as the recyclability potential, would offset the high capital cost typically associated with ILs (Greer, et al., 2021). The extracted metal ions in the IL-organic phase could be removed using an acidic stripping solution. Nakashima et. al (2005) conducted a study using a neutral extractant, octyl(phenyl)-N,N-diisobutylcarbamoylmethylphosphine oxide (CMPO) dissolved in 1-butyl-3-methyl-imidazolium hexaflourophosphate ($[Bmim][PF_6]$). It was reported that aqueous nitric acid solutions were ineffective in stripping the extracted metal ions. A complexing agent (that forms

10

a water-soluble complex with the ions) was added to the acidic solution, with citric acid being the most effective additive, which completely stripped the IL-organic phase. The authors reported no depreciation in the extraction achieved with the recycled IL-organic phase, thus indicating a strong recyclability potential (Nakashima, et al., 2005).

2.3 Measurement Analyses

2.3.1 Distribution Coefficient & Separation Factor

The degree of extraction achieved during separation is indicated by the distribution coefficient. It refers to the ratio of the metal ion concentration, [A], after extraction in organic and aqueous phases respectively, as shown in Equation 2-7 (Gregoric, et al., 2018). The metal ion concentration in the aqueous phase prior to extraction is known, based on the measured quantities used to synthesise the feed solution. The metal ion concentration in the aqueous phase after extraction is determined via ICP-OES analysis, and is discussed further below. Thus, the organic phase metal ion concentration is determined by difference.

$$D_A = \frac{[A]_{organic}}{[A]_{aqueous}} \tag{2-7}$$

The separation factor indicates the relative degree of extraction between two components in the LLE system. For two metals A and B, the separation factor is the ratio of the distribution coefficients of A and B, respectively, as shown in Equation 2-8 (Gregoric, et al., 2018).

$$SF_{A/B} = \frac{D_A}{D_B} \tag{2-8}$$

2.3.2 LLE Equipment

Nayak, et al. (2014) performed the aforementioned measurements using a 5 mL equilibrium tube with 1 mL of each phase, at a constant temperature of 298 K. The distribution ratios reported were quantified by the ratio of radioactivity of the REE in the organic and aqueous phases. The radioactivity of the REEs in each phase was measured using a well-type NaI(TI) detector (Nayak, et al., 2014).

Nascimento, et al. (2015) investigated the effect of the HCL aqueous phase pH (0.2 – 1.4) and HDEHP concentration (0.75 M – 1.5 M), among other variables. Measurements were performed using 50 mL of each phase in an Erlenmeyer flask. A reciprocal shaker (IKA) was used to apply agitation at 250 rpm for 15 minutes at room temperature. Settling occurred for 40 minutes in a separation funnel thereafter (Nascimento, et al., 2015).

2.3.3   Potentiometric Titration Analysis

The nitric acid concentration in the aqueous phase after extraction is determined using potentiometric titration. This method of titration detects the equivalence point with a pH indicator electrode that measures the change in potential across the electrode in terms of the titrant volume added. There are four types of potentiometric titration, in which each type has its own suitable pH electrode (Hulanicki, et al., 2005). In this study, acid/base titration was performed using a known concentration of sodium hydroxide titrant to neutralize and determine the concentration of nitric acid. A glass electrode encasing the reference indicator electrode, typically silver/silver chloride, was used in this application. The cavity of the glass electrode is filled with a solution of chloride ions, typically a potassium chloride solution of constant pH. The bulb of the electrode is made from a sensitive glass membrane, thus allowing the potential difference between the internal solution and the titration sample to be measured, according to the Nernst equation (Glab & Hulanicki, 2005).

2.3.4   ICP-OES Analysis

As mentioned above, the metal ion concentration remaining in the aqueous phase after extraction is experimentally determined using an Inductively Coupled Optical Emission Spectrometry (ICP-OES) apparatus. The device operates on the principle of excited atoms or ions emitting light as their electrons drop from higher to lower energy levels. The wavelength of emitted light is specific to different elements; the amount of light emitted at a particular wavelength is related to the amount of atoms transitioning the energy levels, through the Beer Lambert law (Agilent , n.d.). Hence, the concentration of that element is determined. A schematic of a typical ICP-OES instrument is shown in Figure 2-5 (Boss & Fredeen, 2004).
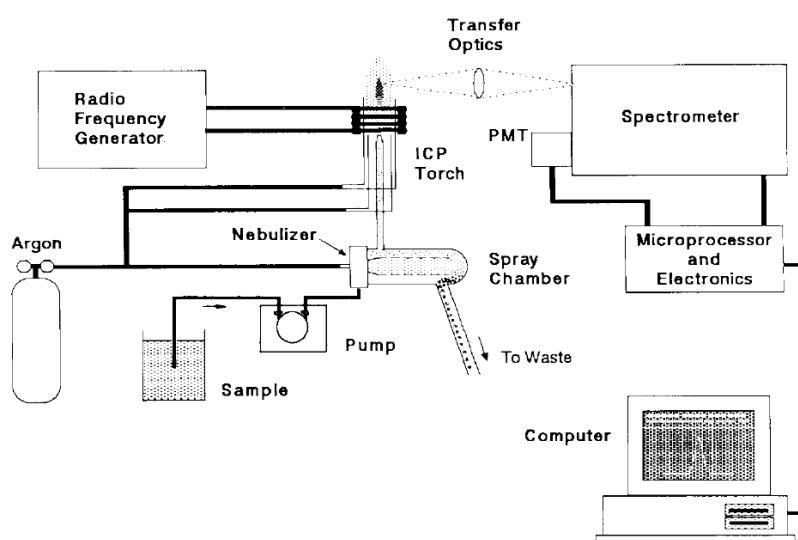
Figure 2-5: Schematic of an ICP-OES instrument (Boss & Fredeen, 2004)

12

A liquid sample to be analysed is fed to the instrument, where it is converted into a fine spray of liquid droplets, known as an aerosol, using the nebulizer. The aerosol is carried into the ICP torch with an argon gas supply. The coil surrounding the torch is connected to a radio frequency generator, which sets up electric and magnetic fields in the vicinity of the torch. This causes electrons to be stripped from the argon molecules, which in turn removes more electrons from the gas, and collide with argon atoms to produce inductively coupled plasma. The plasma removes the solvent from the aerosol, leaving behind salt particles of the sample. The salt is vapourised into gaseous molecules, which are then dissociated into atoms. The atoms are then ionized and excited to emit light of a specific wavelength that is received by the spectrometer. The radiated light is processed into electrical signals that are correlated to the concentration of a particular metal in the sample (Boss & Fredeen, 2004).

If the sample contained multiple elements, light of different wavelengths will be emitted. The recorded emission spectra will show peaks in the emission lines for each element at its characteristic wavelength, thus enabling identification of the elements in the sample, as shown in Figure 2-6 (Agilent , n.d.).
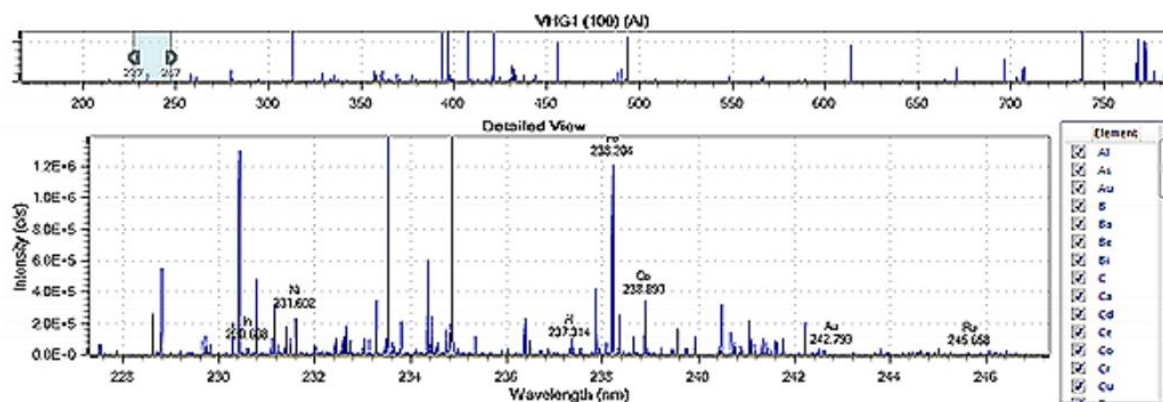
Figure 2-6: Emission spectra of a multi-component sample (Agilent , n.d.)

The concentration of a particular element in the sample is determined using a calibration curve. Multiple standard solutions, containing known concentrations of the element of interest, are prepared and tested by ICP-OES apparatus. The intensity for each standard solution is recorded and plotted against the corresponding standard solution concentration to produce a plot, as shown in Figure 2-7 (Boss & Fredeen, 2004). Thus, the intensity from an unknown sample is matched to the corresponding elemental concentration using the calibration curve.
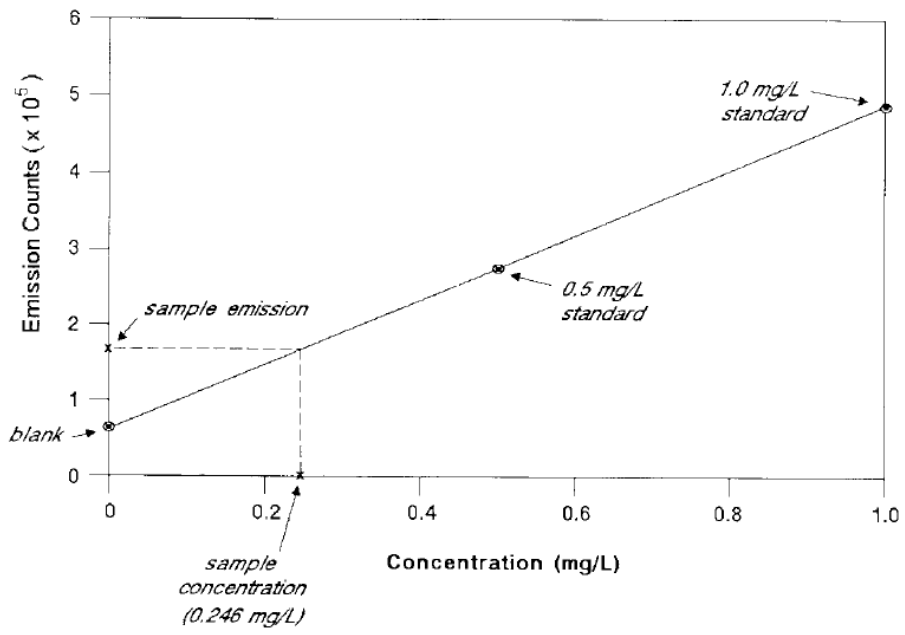
Figure 2-7: ICP-OES calibration curve (Boss & Fredeen, 2004)

3   Methodology

This chapter reports on the materials, apparatus and experimental methods applied in this work. This was followed as per the post-graduate study conducted in parallel.

3.1   Materials

The chemicals used in the experimental work for this study are presented in Table 3-1. These chemicals were used without further purification from the suppliers.

Table 3-1: List of chemicals required for experimental work ✓

Chemical Name	Chemical Formula	CAS Number	Supplier	Purity (wt%)
Bis(2-ethylhexyl) Phosphate "HDEHP"	$C_{16}H_{35}O_4P$	298-07-7	Merck	0.95[a]
Deionised water	H_2O	7732-18-5	Laboratory	[b]
Iron (III) oxide	Fe_2O_3	1309-37-1	BDH	0.85[c]
n-Docedane	$C_{12}H_{26}$	11-40-3	Merck	0.995[a]
Neodymium (III) oxide	Nd_2O_3	1313-97-9	Sigma Aldrich	0.9999
Nitric acid	HNO_3	7697-37-2	Merck	0.55
Potassium hydrogen phthalate	$C_8H_5KO_4$	877-24-7	Merck	0.998
Sodium hydroxide	$NaOH$	1310-73-2	Sigma Aldrich	0.98
Tributylmethylphosphonium methyl sulfate ('IL 1')	$C_{14}H_{33}O_4PS$	69056-62-8	Fluka Analytical	>0.95
Tributylmethylphosphonium tosylate ('IL 2')	$C_{20}H_{37}O_3PS$	374683-35-9	Io-li-tec	>0.95

[a] Volume basis; [b] Electrical resistivity of18MΩ.cm

[c] possible impurities expected in the iron (III) oxide include manganese oxides, silica and clay.

3.2   Equipment

The main apparatus required to perform the experiments is a bench-scale LLE setup, as shown in Figure 3-1.

<div align="center">

Student 1 Measurements   Student 2 Measurements

(Riyantha Moodley)   (Sohana Bridgemohan)
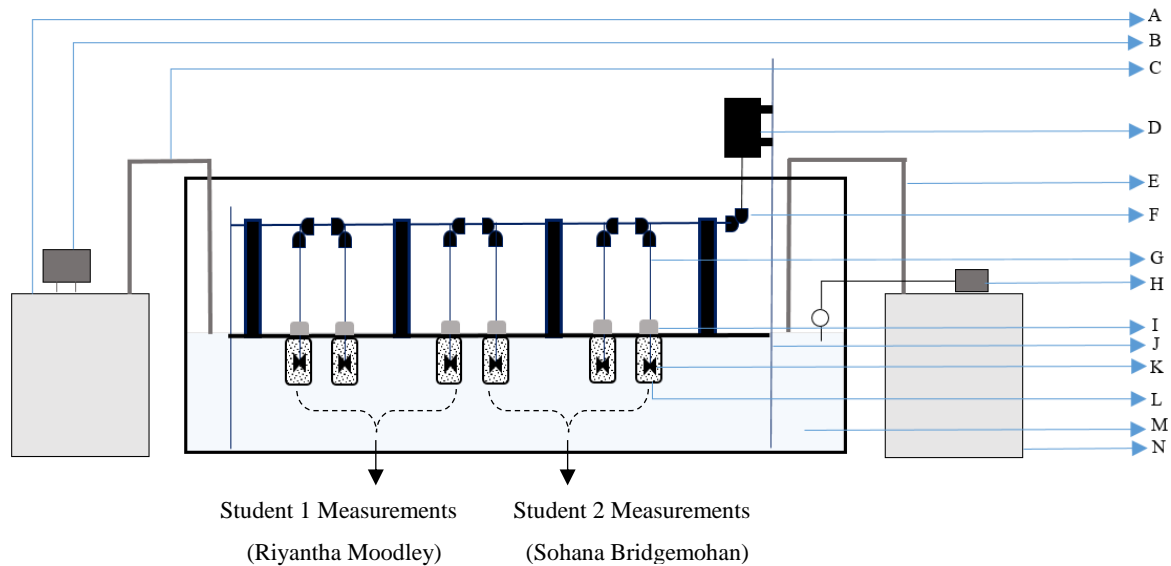
Figure 3-1: Schematic of bench-scale LLE apparatus

</div>

A-controlled heater, B-heater temperature control and display, C-hot water supply to water bath, D-motor, E-cold water supply to water bath, F-gear, G-mixer shaft, H-water bath temperature display connected to Pt100 probe, I-test compartment lid (mounted to metal platform support on the LLE apparatus frame), J-LLE apparatus frame, K-mixer blade, L-test compartment body, M-water bath, N-controlled chiller.

A schematic of the bench-scale LLE apparatus is illustrated in Figure 3-1. This apparatus was used to enable the metal ion extraction of interest during each experimental run. The main metallic framework (J) contains a gear shaft that drives 6 different mixer shafts (G). Each mixer shaft is fitted with an agitator or mixer (K) to facilitate vigorous mixing of each of the separate 10 mL test compartments (L). The shafts are driven by a motor (D). The motor is connected to a power supply, with an attached timer (not shown in the Figure) to automatically start and end the agitation. The apparatus frame is placed within a water bath, the walls of which are transparent, to allow observation of the apparatus during operation. The water bath temperature is monitored via a Pt100 sensor, connected to a display (H). The temperature of the water bath is regulated with a controllable heater and chiller (A and N, respectively). The temperature of the separate water bath within the heater is manually adjusted at the temperature control (indicated by B). The lids of each test compartment (I) are fixed to the metallic framework, to allow easy mounting and dismounting of the test compartments. Each lid has two access ports – one is an access point for the mixer shaft, while the other is a sampling point.

In this work, a mixing and settling time of 12 and 8 hours was recommended and applied, respectively (Bayeni, 2021). These times were based on pre-determined values, obtained by trial and error.

✓

The additional measurement devices, and their relevant specifications, are listed in Table 3-2. In the absence of manufacturer uncertainties, an appropriate estimate was used and indicated where applicable.

Table 3-2: Measurement devices and specifications

Device	Brand/Model	Specifications
Analytical mass balance	Ohaus, Adventurer	Readability: 0.00001g Uncertainty: ±0.0006g
Potentiometric titrator	Metrohm Titrando, 888	Readability: 0.0001 mol/L Uncertainty: ±0.0001 mL
ICP-OES	Perkin Elmer Optima 8300	Calibration uncertainty to follow for each run
Micropipette (1000-5000µL)	IsoLab	Uncertainty: ±0.02 mL (Artel, 2016)
Micropipette (100-1000µL)	IsoLab	Uncertainty: ±0.02 mL (Artel, 2016)
Pt 100 temperature sensor	Wika	Display readability: 0.1°C Uncertainty: ±0.14°C

✓

The list of auxiliary equipment and resources used are listed:

- Ethanol cleaning solution
- Centrifuge tubes, of 15 mL and 50 mL capacity
- NaOH stock solution (0.029615 M was used in this study)
- Spatula, funnel and plastic dropper
- Syringe with a 10 cm needle
- Glassware: Erlenmeyer flasks (25 mL,100 mL), funnel and measuring cylinders (25 mL, 100 mL)
- Consumables: micropipette fittings (1000 µL and 5000 µL capacity)
- Barometer (Mensor, CPC 3000)

3.3 Experimental Procedure

The experimental work comprised of four experimental runs that were aligned to the objectives of this investigation, as indicated in Table 3-3. All measurements were conducted at a fixed temperature of 25°C and pressure of 1 atm.

Table 3-3: Overview of Experimental Work

Run	Aqueous Phase	Organic Phase
1 (test system)	Nitric acid (0.1M, 0.5M, 0.9M) Nd_2O_3 (2000ppm) Deionized water	HDEHP (0.5M) n-Dodecane
2	Nitric acid (0.1M, 0.5M, 0.9M) Fe_2O_3 (2000ppm) Deionized water	HDEHP (0.5M) n-Dodecane
3	Nitric acid (0.1M, 0.5M, 0.9M) Fe_2O_3 (2000ppm) Deionized water	HDEHP (0.5M) Ionic liquid (0.1M) * n-Dodecane
4	Nitric acid (0.1M, 0.5M, 0.9M) Deionized water Nd_2O_3 + Fe_2O_3 (30:70 ratio, total loading of 2000ppm)	HDEHP (0.5M) n-Dodecane

*Both IL 1 (tributylmethylphosphonium methyl sulfate) and IL 2 (tributylmethylphosphonium tosylate) investigated

The experimental procedure is divided into three consecutive steps: solution preparation, extraction and analysis. The procedure described for these three steps were performed for all experimental runs, and were modified to accommodate the variable investigated in each run (the addition of ionic liquid in the organic phase, or the specific metal oxide used, etc.)

18

3.3.1   Solution preparation

Aqueous feed solutions:

The feed solutions were prepared using pre-determined quantities (mass basis) of the respective solute, solvent and diluent. The required masses are indicated in Table D-1 in Appendix D.1, the sample calculation for which is presented as well. The preparation method is as follows:

1. A 100 mL Erlenmeyer flask was placed on the mass balance. The weight was recorded and the balance was tared.

2. Using a spatula, the required metal oxide powder mass was added to the flask. The mass was recorded and the balance was tared.

3. Using a glass cylinder and funnel, the required mass of nitric acid was added to the flask. As the mass approached the desired value, a dropper was used for improved accuracy. The mass was recorded and the balance was tared.

4. Step 3 was repeated with deionized water.

5. The flask was sealed and agitated.

6. The feed solution was then dispensed into a 50 mL centrifuge tube for storage.

Organic feed solutions:

An analogous procedure described to prepare the aqueous feed was performed using the required constituent components: HDEHP, n-dodecane and ionic liquid (where necessary). The required organic phase masses are indicated in Table D-2 in Appendix D.1.

ICP-OES standard solutions

The aqueous feed solution (at any nitric acid concentration) was successively diluted to produce ICP standard solutions. Metal loadings at 100, 80, 50, 20, 9, 7, 5, 3 and 1 ppm were prepared, according to the volumes listed in Table D-3 in Appendix D.1. The method is as follows:

1. The required volume (V_1) from the concentrated solution (C_1) was dispensed using a micropipette into an Erlenmeyer flask.

2. Deionised water was added to the flask until the desired volume (V_2) that corresponds to the desired metal loading (C_2), was reached.

3. The flask was sealed and agitated.

4. A 15 mL sample of this standard solution was dispensed into a 15 mL centrifuge tube.

5. The solution was reserved and successively diluted according to steps 1-4, until all standard solutions for all concentrations were prepared.

19

3.3.2   Extraction

Each experiment contained three nitric acid concentrations (0.1 M, 0.5 M, and 0.9 M). Measurements for each concentration were duplicated and performed independently by each student, to test the repeatability reproducibility of the results. Thus, a total of six measurements were obtained in each experimental run. The method for extraction is as follows:

1. The water bath was prepared: the main apparatus and heater baths were filled to an appropriate predetermined level. The heater was switched on, with its set point at the recommended value. The chiller and pump were switched on. This ensured that the bath temperature in which the cells were housed was approximately 25°C. The Pt100 probe was place into the bath.

2. The glass test compartment/vial was placed on the analytical mass balance, and its mass was recorded.

3. The aqueous feed solution was agitated in its centrifuge tube.

4. Using a micropipette, 5 mL of the aqueous feed was drawn and dispensed into the glass vial.

5. The mass of the aqueous phase was recorded, and the balance was tared.

6. The organic feed was dispensed on top of the aqueous phase, according to steps 3-5.

7. Steps 2-5 were repeated for all 6 test vials for each nitric acid concentration.

8. Each test compartment was screwed onto the LLE apparatus frame, ensuring that the correct vials were attached to the correct position on the frame, according to Figure 3-1. Student 1's vials (0.1 M, 0.5 M, 0.9 M HNO_3) occupied the first 3 positions on the apparatus and Students 2's (the author's) vials (duplicate 0.1M, 0.5M, 0.9M HNO_3) occupied the last 3 positions on the apparatus.

9. The stabilized water bath temperature and barometric pressure in the room was recorded.

10. The apparatus frame was lowered into the water bath.

11. The timer was set to ensure mixing occurred for 12 hours.

12. An 8 hour settling period was allowed to pass.

3.3.3   Sampling & Analysis

Sampling

The sampling method is described as follows:

1. A syringe, fitted with a 10 cm needle, was carefully inserted through the vial sampling point and the settled organic layer, such that it was touching the bottom of the vial.
2. The syringe plunger was steadily drawn so as to not disturb the miscibility boundary between the settled phases. The settled aqueous phase was withdrawn from the vial until the meniscus boundary began to touch the bottom of the vial.
3. The extracted aqueous phase was dispensed into a 15mL centrifuge tube for storage.
4. Steps 2-4 were repeated for all 6 vials on the frame.
5. Using a micropipette, 1mL of the extracted aqueous phase was dispensed into a fresh Erlenmeyer flask.
6. The flask was filled to capacity with deionised water, thus diluting the aqueous phase.
7. The flask was sealed and agitated.
8. A 15 mL sample of this diluted aqueous phase was dispensed into a centrifuge tube for ICP-OES analysis.
9. The masses of two 50 mL centrifuge tubes were recorded.
10. 25mL of the diluted aqueous phase was dispensed into these centrifuge tubes for titration analysis.
11. Steps 6-11 were repeated for all extracted aqueous phase samples.

Note that between each withdrawal from the test compartments, the syringe was cleaned thoroughly. Three washes with deionised water, followed by two washes with ethanol cleaning solution, were performed. The liquid was drawn with the plunger at the end of the syringe and agitated, to clean the entire syringe cavity. The used cleaning solutions were dispensed into a waste bottle. The needle was wiped with a wetted tissue: thrice with deionised water, and twice with ethanol.

ICP-OES Analysis

The prepared ICP standard solutions, as well as the diluted aqueous phase samples obtained from each experiment were delivered to the Department of Chemistry (PMB Campus, UKZN) for ICP-OES analysis.

Titration analysis

Six aqueous phases (one per extraction cell) were extracted and diluted in each run. From each diluted phase, two samples were drawn for titration analysis. Thus, a total of twelve titration samples were analysed per experimental run. The method is as follows:

1. The desktop PC that houses the titration interface (Metrohm Titrando, 888) was switched on.

2. A magnetic stirrer bar was placed in the NaOH titrant bottle, with its stirrer pad switched on.

3. A waste beaker was placed on the sampling pad. The burette tip was positioned over the beaker.

4. The existing titrant in the titrant vessel was discharged into the waste beaker and replaced with fresh NaOH titrant from the bottle. The beaker was removed, and the spent titrant was discarded.

5. The mass of the centrifuge tube containing the aqueous phase was measured using an analytic balance and recorded. Using the empty tube mass recorded prior, the mass of the diluted sample was calculated by difference. The sample mass and approximate molarity* was entered as an input to the software interface.

6. The sample was agitated before analysis.

7. The tube lid was removed, and another magnetic stirrer bar was added to the sample. The tube was placed upright in a separate beaker (for support), and was placed onto the sample pad of the titration apparatus.

8. The pH meter and the burette tip were inserted into the centrifuge tube.

9. The titration was prompted using the software, and continued until the equivalence point was reached.

10. The reported NaOH titrant volume that was delivered during the titration was recorded.

11. Steps 5-10 were repeated for all diluted aqueous samples, with the stirrer bar removed and wiped with a tissue wetted with deionised water between titration analyses.

12. The H^+ concentration of the sample was thus calculated.

✓

Note that the approximate molarity follows from the aqueous feed of either 0.1 M, 0.5 M or 0.9 M. Accounting for the dilution of the extracted aqueous phase, the approximate molarity entered into the interface was thus either 0.001 M, 0.005 M or 0.009 M.

3.4   Hazard Evaluation & Safety Precautions

3.4.1   Chemical Hazards

The Material Safety Data Sheets (MSDS') were consulted prior to all experimental work commenced. It was found that the metal oxide powders can cause irritation of the respiratory tract if dusts are inhaled (Scholar Chemistry, 2009; Sigma-Aldrich, 2018). Both nitric acid and the ionic liquids were found to be harmful upon contact with the skin, and present vapour/mist inhalation hazards (Santa Cruz Biotechnology, 2017; ThermoFisher Scientific, 2019). HDEHP also poses a contact hazard (Sigma-Aldrich, 2019).

3.4.2   Equipment Hazards

The power supply for the motor, heater and chiller from the LLE apparatus was located near the water bath. Thus care was taken to ensure water spillages were cleaned promptly, if any. Deionised water and ethanol were used to clean all glassware, equipment and surfaces in contact with the liquid mixtures. All washing solutions and used chemicals were discarded in an allocated waste bottle.

3.4.3   Personal Protective Equipment

Two layers of gloves were worn: latex and nitrile gloves. Safety glasses, a laboratory coat and safety boots were worn as per standard laboratory practice. A face mask was also worn.

4   Results

The distribution ratios of neodymium and iron over the investigated nitric acid concentration range are presented in Figures 4-1, 4-2 and 4-3, for runs 1, 2 and 4, respectively. The corresponding measurements as produced by the author, Student 2 (Sohana Bridgemohan), are presented in Table 4-1. The separation factor (SF) is indicated for the final experimental run in which a combined metal oxide system was used.

Table 4-1: Distribution Coefficients (D) & Separation Factor (SF) of Nd and Fe from aqueous HNO_3 solutions (0.1 M, 0.5 M, 0.9 M) using 0.5 M HDEHP in n-dodecane.

Run	T [°C]	P [kPa]	Feed [HNO₃] [M]	Titrated [HNO₃] [M]	D_{Nd}	D_{Fe}	$SF_{Nd/Fe}$
1	25.20	100.090	0.0969	0.0777	10.674[a]		
			0.500	0.252	3.993[a]		
			0.896	0.367	1.075[a]		
2	24.55	100.305	0.105	0.145		20.371[b]	
			0.512	0.396		21.915[b]	
			0.918	0.357		15.313[b]	
4	21.45	99.605	0.106	0.114	N/A	14.161[d]	N/A
			0.507	0.380	1.321[c]	13.726[d]	0.507
			0.904	0.655	0.656[c]	13.644[d]	0.904

Runs 1: neodymium; 2: iron; 4: neodymium and iron

[a] combined standard uncertainty, u_c (θ) = 1.161;
[b] combined standard uncertainty, u_c (θ) = 0.594;
[c] combined standard uncertainty, u_c (θ) = 1.710;
[d] combined standard uncertainty, u_c (θ) = 1.807

The results from runs 1, 2 and 4 are combined with the distribution ratios of neodymium produced in the post-graduate study that was conducted in parallel to this investigation, in Figure 4-4 (Bayeni, 2021).
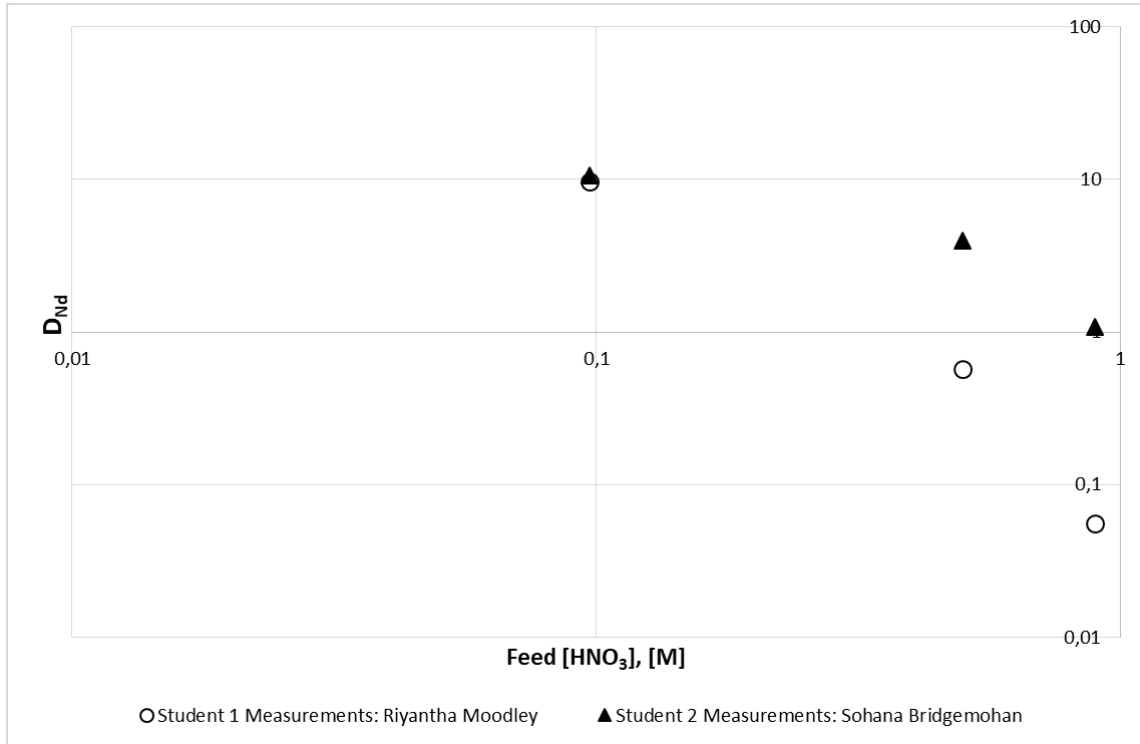
Figure 4-1: Distribution ratio of neodymium over the HNO_3 feed concentration range [M] – Run 1 (Test system) 0.5M HDEHP (n-dodecane); T= 25.2 °C, P = 100.09 kPa. Combined standard uncertainty in $D_{Nd:}$, u_c (θ) = 1.161
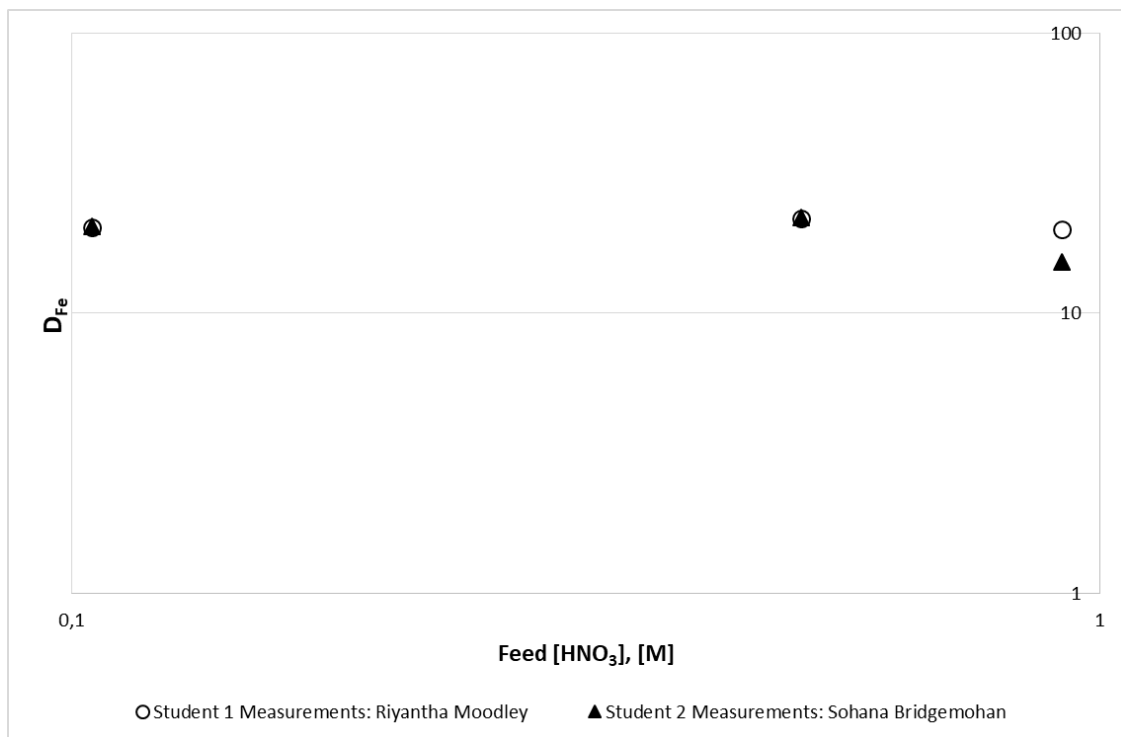
Figure 4-2: Distribution ratio of iron over the HNO_3 feed concentration range [M] – Run 2 0.5M HDEHP (n-dodecane); T= 24.55 °C, P = 100.31 kPa. Combined standard uncertainty in D_{Fe}, u_c (θ) = 0.594

25
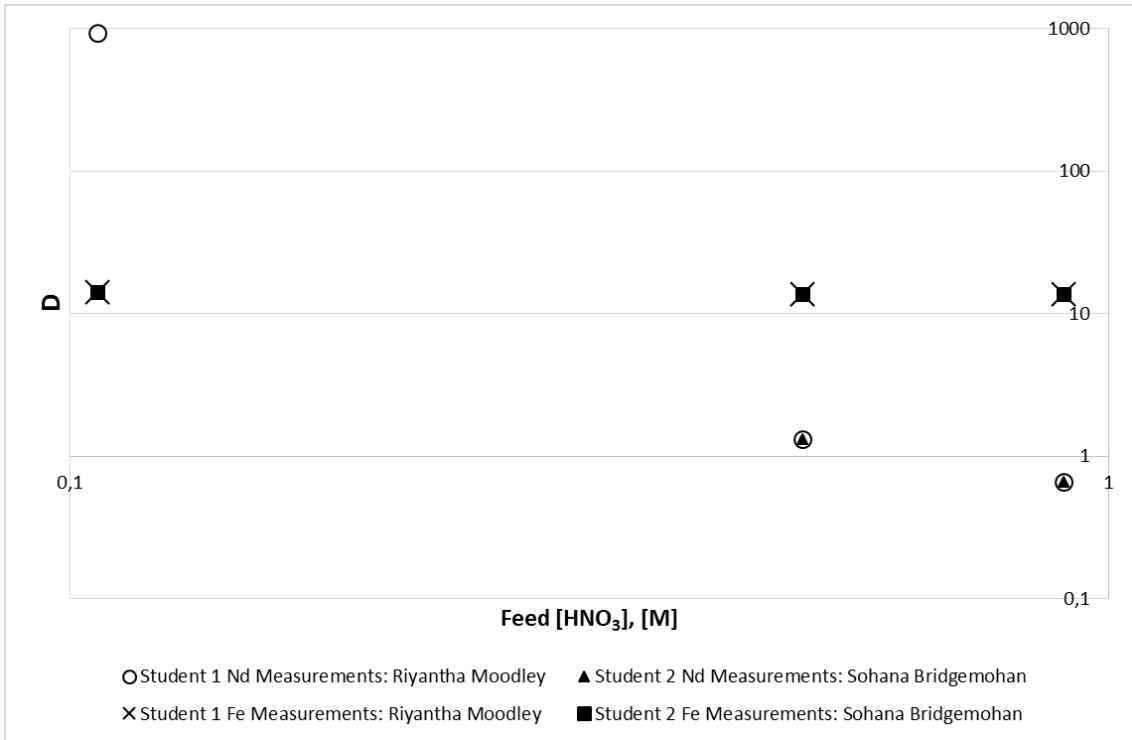
Figure 4-3: Distribution ratios of iron and neodymium over the HNO_3 feed concentration range [M] – Run 4 0.5M HDEHP (n-dodecane); T= 21.45 °C, P = 99.61 kPa. Combined standard uncertainty in D_{Nd}: u_c (θ) = 1.710, Combined standard uncertainty in D_{Fe}: u_c (θ) = 1.807
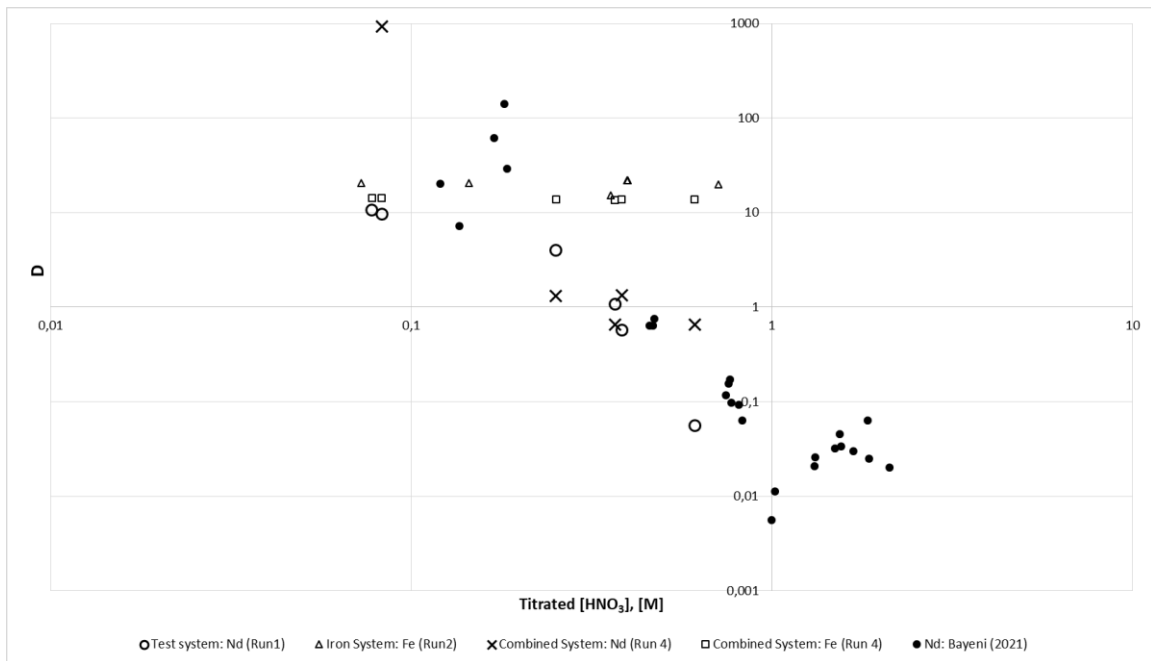
Figure 4-4: Distribution ratios from all runs overlapped with Extraction of Neodymium data (0.5 M HDEHP) (Bayeni, 2021) against the titrated HNO_3 concentration [M]

The experiment pertaining to the effect of ionic liquid doping on the system could not be performed, due to phase splitting that occurred in the organic phase, as shown in Figure 4-5. Hence the distribution ratio of iron during run 3 was not determined. This occurred with both IL 1 (tributylmethylphosphonium methyl sulfate) and IL 2 (tributylmethylphosphonium tosylate).

Split IL phase
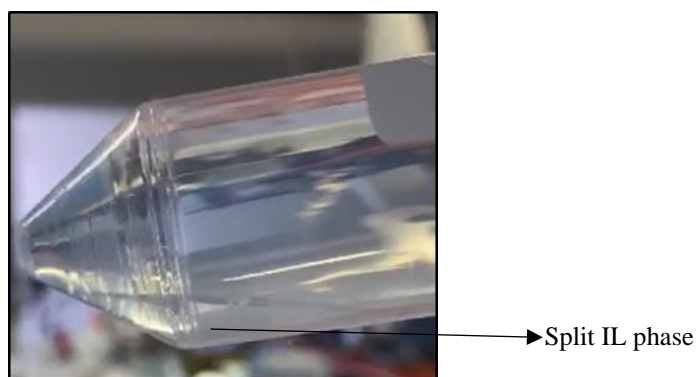
Figure 4-5: Split organic phase during IL doping: 0.1 M IL1 with 0.5 M HDEHP in n-dodecane (Run 3)

5   Discussion

The distribution ratios of neodymium in the test system were successfully determined across the nitric acid concentration range of interest (0.1 M, 0.5 M and 0.9 M). The distribution ratio of neodymium was inversely proportional to the nitric acid concentration, as seen in Figure 4-1, where the distribution was highest at 10.674, in a feed concentration of 0.1 M. This is consistent with the theory of rare earth extraction using acidic extractants, such as HDEHP, wherein the degree of extraction is favoured in acidic solutions at higher pH's (Xie, et al., 2014). Furthermore, this trend in the data is consistent with that reported by Nayak, et al. (2014) in Figure 2-3, as well as that produced by Bayeni, T (2021) in Figure 4-4, for the same liquid-liquid system. The consistency between the measured and reported extraction data indicates the successful verification of the experimental method used in this study. There is a notably good agreement with the data produced by Student 1, though some discrepancy in the duplicate measurements is observed at the 0.5M and 0.9M concentrations, as seen in Figure 4-1.

The distribution ratios of iron over the nitric acid concentration range are illustrated in Figure 4-2. The figure illustrates an approximately constant distribution of iron across the entire range. The numerical results from Table 4-1 indicate that the distribution ratio of iron decreased from 20.371 (at 0.1 M) to 15.313 (at 0.9 M), conforming to the aforementioned trend observed for the neodymium extraction. However, the increase in the intermediate distribution at 0.5 M, as well as the scatter in the duplicate distribution measurements at 0.9 M do not support this inversely proportional trend. To the best of the author's knowledge, no literature is available on the extraction of iron alone in solution; hence, a comparison to existing work cannot be made to verify the validity of the results. Thus, it is proposed that the extraction of iron by 0.5M HDEHP in n-dodecane is virtually unaffected by variations in the nitric acid feed concentration, and remains fairly constant in the high pH range.

The investigation into the effect of doping with an IL (tributylmethylphosphonium methyl sulfate) at 0.1 M on the distribution ratio of iron was not performed, due to the occurrence of phase-splitting, shown in Figure 4-5. A second phosphonium-based IL, tributylmethylphosphonium tosylate, was available, hence another organic phase sample was prepared, in the same concentration, to assess the resulting phase behaviour. Phase splitting occurred as with the previous sample, in which the viscous IL settled out of the solution. Thus,

both organic phase samples were not usable since, despite agitation, a uniform concentration of IL in each dispensed organic phase across the test compartments could not be maintained. The third liquid phase would also complicate the hydrodynamics of the LLE system; the analysis of which, is beyond the scope of this investigation. Other phosphonium based ILs reportedly have an affinity for non-polar solvents due to bulky substituent groups surrounding the central phosphorus atom, reducing their intermolecular columbic forces of attraction (Banerjee & Khanna, 2006; Carvalho, et al., 2014). Additionally, no phase splitting between ILs and extractants has been reported in existing literature, suggestive of their mutual solubility. Hence, the molecular interactions between the n-dodecane solvent, HDEHP extractant, and IL used will require further investigation to understand the phase immiscibility.

Consequently, a fourth experimental run was performed, in which the extraction from a combined iron and neodymium oxide aqueous phase was investigated. The aqueous feed contained a total metal loading of 2000 ppm, similar to that of the previous experimental runs, with an iron/neodymium ratio of 70/30 on a mass basis, as this is the typical composition of NdFeB magnets (Tunsu, et al., 2015). The iron distribution remained relatively constant across the acid concentration range (D_{Fe}: 13.644 – 14.616), with a combined uncertainty of 1.807. The inversely proportional relationship between the distribution of neodymium and nitric acid concentration strengthened, compared to the test system of run 1, as seen in Figure 4-4. For example, the neodymium distributions at 0.5 M nitric acid decreased from 3.933 in run 1 (pure neodymium system) to 1.321 in run 4 (iron and neodymium system). This variation in extraction behaviour presents an opportunity to exploit the higher distribution ratios of neodymium in the dilute acid concentration range, to obtain a high separation factor.

The distribution of neodymium and the corresponding separation factor at 0.1 M for Student 1 was 926.947 and 65.633, respectively, as reported in Table D-7 (Appendix D.3). The post-extraction samples were analysed in triplicate for the detection of neodymium, from which the average values were taken. For samples in which "undervalue" results were received, the data was omitted. However, for the neodymium system at the 0.1 M acid concentration, the sample (i.e., the author's measurement) persistently reported as undervalue, thus is absent from the data. This error is possibly related to the calibration of the ICP device, wherein the range of concentrations used in the calibration may have been too wide. The absolute errors in the higher concentration region would have more strongly influenced the least-squares fitting used to

generate the linear calibration curve (PerkinElmer, 2018). Hence, a poor fit in the dilute concentration region of interest would occur, resulting in undervalue measurements. This is justified by the reported calibrations listed Tables C-11 to C-13 (Appendix C.5): calibration standards ranged from 0 ppm (blank)–150 ppm, while all measured neodymium concentrations were in the extremely dilute range (less than 5 ppm).

Given the excellent reproducibility of the remaining duplicate measurements in run 4, it is likely that the distribution ratio of neodymium (0.1 M nitric acid) would have resulted in a fairly similar result as that of Student 1. Additionally, the reported undervalue ICP concentration at 0.1M invariably indicates an especially low post-extraction neodymium concentration, which supports the enhanced rare earth extraction observed at this dilute acid concentration. Evidently, HDEHP is more selective towards neodymium at nitric acid concentrations less than 0.5 M, which is supported by the REE complex formation being favoured at higher pH's (Gregoric, et al., 2018).

Figure 4-4 displays all the results obtained in this study, against the neodymium extraction data from the associated postgraduate study by Bayeni (2021). The constant distribution ratio of iron across the acid concentration range is evident, with that in the combined metal oxide system (run 4) being lower than that in the 'pure' iron system (run 2). This may be explained by the reduction in HDEHP extraction sites available to Fe^{3+} due to competing Nd^{3+} ions present in solution. The neodymium distribution in runs 1 and 4 shows good agreement with the trend displayed by Bayeni (2021). There is currently no reported work in which the effect of varying acid concentration on the distribution of iron and neodymium (in a combined system) is investigated using a cationic extractant, with which to compare the results.

According to the cationic extraction mechanism in Equation 2-4, it was anticipated that the nitric acid concentration would increase as H^+ ions are transferred into the aqueous phase during extraction. However, the results in Table 4-1 indicate that acid concentration decreased after extraction in all experimental runs. It has been established that the observed trend in the distribution ratio of neodymium is consistent with that published in literature. Hence, this decrease in the acid concentration is most likely the result of an error in the known concentration of the NaOH titrant, since an existing titrant solution was used in these analyses.

The iron oxide used in this investigation was of a low purity, at 85%. Samples of this purity were used, due to the late delivery of the required chemicals purchased for this project. Hence, to avoid delays to the experimental work plan, this iron oxide sample was sourced from the Chemical Engineering Department. It is possible that impurities in the oxide (possibly manganese oxides, silica or clay) inhibited the extraction of iron (competing for extraction sites), hence a true reflection of the extraction behaviour of iron has, most likely, not been observed. However, WEEE material will form the feed of the hydrometallurgical recycling process of interest, thus there will invariably be impurities present from the leaching phase, prior to extraction. Thus, the trends observed in the iron distribution over the nitric acid concentration range are still informative and provide a useful source of data.

Based on the aforementioned trends, it is clear that HDEHP at 0.5 M in n-dodecane exhibits a strong selectivity for neodymium at dilute acid concentrations, where the highest separation factor of 65.633 was observed at 0.1M HNO_3 (by Student 1). However, the extraction may be improved by increasing the HDEHP concentration as shown by Gregoric, et al. (2018) in which this was observed in acetic- and citric acid systems. In conjunction with the aforementioned distribution behaviours, the relatively cheap cost and availability of HDEHP adds to the attractiveness of this separation method on a commercial scale (Gruber & Carsky, 2020).

In a pilot scale leaching, and two-step continuous LLE process, Gruber & Carsky (2020) investigated the potential of a vibrating plate column to extract praseodymium and neodymium oxides from spent NdFeB magnets. Sulphuric acid (1.5-2M) and HDEHP (40% v/v) in n-dodecane comprised the liquid-liquid system, from which a yield in excess of 95% and a minimum rare earth oxide purity of 99% was obtained. Evidently, the excellent performance reported by the authors is a strong indication of the potential for this separation method within the overall recycling process. The contributions from this investigation may further inform future pilot-scale studies to improve the performance, by operating in the dilute acid concentration range. However, LLE does not exist in isolation in this hydrometallurgical process: the optimum conditions of the upstream leaching process will also be considered. Hence, a trade-off is likely to exist between operating in the dilute acid concentration region to promote rare earth extraction (and hence the product purity) and operating with highly concentrated acidic solutions to improve the leaching efficiency, and thus the overall recovery of the process (Gregoric, et al., 2018).

6   Conclusion

The test system results indicated that the distribution ratio of neodymium is inversely proportional to the nitric acid concentration, where the highest neodymium distribution of 10.674 was observed in the 0.1 M nitric acid sample. This trend is consistent with that reported in the literature for the same liquid-liquid system, and with the acidic nature of the HDEHP extractant. The distribution ratio of iron over varying nitric acid concentrations (0.1M - 0.9M), using 0.5 M HDEHP in n-dodecane, was observed to be relatively unaffected by variations in the nitric acid concentration and remains approximately constant in the region of 20.

Phase splitting in the organic phase containing 0.1 M of ionic liquid and 0.5 M of HDEHP occurred. Thus, the distribution ratio of iron in this LLE system was not measured. The nature of molecular interactions between all 3 components in the organic phase that promoted phase splitting was unclear, and is to be investigated further. The extraction of iron and neodymium from a combined metal oxide system displayed consistent behaviour with the results from previous experiments pertaining to the individual metals. The highest separation factor of 65.633 was observed at the lowest nitric acid concentration investigated (0.1 M).

The uncertainties of measurement and the ICP calibration uncertainties comprised the combined standard uncertainty for each experimental run. The author's neodymium concentration at 0.1M in the combined metal oxide system was reported as undervalue. It was proposed that this was due to too wide a range of standard concentrations used to calibrate the ICP device, resulting in a poor linear fit in the dilute metal loading region of interest. Overall, excellent reproducibility was observed in the duplicate measurements, particularly in the iron and combined metal oxide systems. The titrated nitric acid concentrations were lower than their corresponding feed concentrations; this erroneous result is likely due to an incorrect reported concentration of the existing NaOH titrant used in this study.

The findings in this work indicate the potential for recovery of neodymium from aqueous solutions of dissolved metals. The design considerations for a commercial-scale process of this nature was discussed, with reference to results from a similar LLE system used in a pilot-scale process from literature.

7   Recommendations

It is recommended that the iron oxide used in the experiments is of a higher purity, to assess the true distribution ratio of iron over the nitric acid concentration range, without the possibility of impurities impairing the distribution and thus skewing the results. Repeat measurements of the experimental runs conducted to rigorously assess the reproducibility of the results is recommended. The reproducibility of the iron oxide and combined metal oxide systems are of particular interest, since there is no knowledge of existing data published for the same liquid-liquid system studied in this work.

Multiple calibration measurements of ICP standard solutions are recommended to improve the accuracy of the calibration, and thus the resulting distribution ratios. It is recommended that more calibration standards are used in the dilute metal loading range (up to 20 ppm) to refine the linear fit of the calibration curve. Additionally, when expecting post-extraction aqueous phase concentrations to be low, it is recommended that a narrow range of standards in that dilute metal loading range are used, to more accurately calibrate the ICP instrument.

Given the reported improvement in the extent and selectivity of separation through ionic liquids, the effect of doping the organic phase should be pursued for the potential to minimize the capital cost in optimizing separations, through smaller quantities of these chemicals. Hence, an investigation into the molecular interactions and affinities for n-dodecane and HDEHP of the phosphonium-based ionic liquid tested in this study, is recommended for future work. Thus, the limitations of phase splitting may be circumvented without wasting chemical reagents, to ultimately investigate the effect of ionic liquid doping on the distribution ratio of iron, which was not achieved in this work.

The objectives completed in this work may be extended to a 1M HDEHP in n-dodecane organic phase, to explore the effect of a higher extractant concentration on the results, which may be compared to the findings in this work. An investigation into the distribution ratio of boron in the same liquid-liquid system, followed by that of powdered NdFeB magnets is recommended to understand the distribution of boron, as well as the selectivity of the HDEHP extractant, over the tested nitric acid concentration range.

8 References

Agilent , n.d. *ICP-OES FAQ's including The ICP-OES Principle, ICP-OES Instrument and ICP-OES Analysis.* [Online]
Available at: https://www.agilent.com/en/support/atomic-spectroscopy/inductively-coupled-plasma-optical-emission-spectroscopy-icp-oes/icp-oes-instruments/icp-oes-faq#:~:text=The%20ICP%2DOES%20principle%20measures,a%20calibration%20curve%20is%20created.
[Accessed 12 May 2021].

Artel, 2016. *Lab Report 5: Setting Tolerances for Pipettes in the Laboratory.* [Online]
Available at: https://www.artel.co/learning_center/setting-tolerances-for-pipettes-in-the-laboratory/
[Accessed 13 May 2021].

Balaram, V., 2019. Rare earth elements: A review of applications, occurence, exploration, analysis, recycling, and environmental impact. *Geoscience Frontiers,* 10(4), pp. 1285-1303.

Banerjee, T. & Khanna, A., 2006. Infinite Dilution Activity Coefficients for Trihexyltetradecyl Phosphononium Ionic Liquids: Measurements and COSMO_RS Prediction. *Journal of Chemical Engineering Data,* Volume 51, pp. 2170-2177.

Batchu, N. & Binnemans, K., 2018. Effect of the diluent on the solvent extraction of neodymium(III) by bis(2-ethylhexyl)phosphoric acid (D2EHPA). *Journal of Hydrometallurgy,* Volume 177, pp. 146-151.

Bayeni, T., 2021. *Extraction of Neodymium. Project title. MSc.Eng. thesis (in progress),* Durban, South Africa.: School of Engineering, University of KwaZulu-Natal.

Binnemans, 2007. Lanthanides and Actinides in Ionic Liquids. *Chemical Reviews,* 107(6), pp. 2592-2614.

Binnemans, K., Jones, P.T., Blanpain, B., Van Gerven, T., Yang, Y., Walton, A. & Buchert, M., 2013. Recycling of rare earths: a critical review. *Journal of Cleaner Production,* Volume 51, pp. 1-22.

Boss, C. & Fredeen, K., 2004. *Concepts, Instrumentation and Techniques in Inductively Coupled Plasma Optical Emission Spectrometry.* 3 ed. s.l.:PerkinElmer.

Carvalho, P.J.; Ventura, S.P.M.; Batista, M.L.S.; Schroeder, B.; Goncalves, F.; Esperenca, J.; Mutelet, F. & Coutinho, J.A.P., 2014. Understanding the impact of the central atom on the ionic liquid behaviour: Phosphonium vs ammonium cations. *The Journal of Chemical Physics,* Volume 140.

Dent, P., 2012. Rare earth elements and permanent magnets (invited). *Journal of Applied Physics,* 111(7).

Ferreira, A., Simoes, P. & Ferreira, A., 2012. Quarternary phosponium-based ionic liquids: Thermal stability and heat capacity of the liquid phase. *Journal of Chemical Thermodynamics,* Volume 45, pp. 16-27.

Glab, S. & Hulanicki, A., 2005. Ion-Selective Electrodes: Glass Electrodes. In: P. Worsfold, A. Townshend & C. Poole, eds. *Encyclopedia of Analytical Science.* s.l.:Elsevier, pp. 498-502.

Goodenough, K., Wall, F. & Merriman, D., 2018. The Rare Earth Elements: Demand, Global Resources, and Challenges for Resourcing Future Generations. *Natural Resources Research,* Volume 27, pp. 201-216.

Greer, A., Jacquemin, J. & Hardacre, C., 2021. Industrial Applications of Ionic Liquids. *Molecules ,* Volume 25, p. Article number 5207.

Gregoric, M., Barrier, A. & Retegan, T., 2018. Recovery of Rare-Earth Elements from Neodymium Magnet Waste Using Glycolic, Maleic, and Ascorbic Acids Followed by Solvent Extraction. *Journal of Sustainable Metallurgy,* Volume 5, pp. 85-96.

Gregoric, M., Ekberg, C., Foreman, M.R.S.J., Steernari, B.M. & Retegan, T., 2017. Characterization and Leaching of Neodymium Magnet Waste and Solvent Extraction of Rare-Earth Elements using TOGDA. *Journal of Sustainable Metallurgy,* Volume 3, pp. 638-645.

, 2017. Characterization and Leaching of Neodymium Magnet Waste and Solvent Extraction of Rare-Earth Elements using TOGDA. *Journal of Sustainable Metallurgy,* Volume 3, pp. 638-645.

Gregoric, M., Ekberg, C., Steenari, B. & Retegan, T., 2017. Separation of Heavy Rare-Earth Elements from Light Rare-Earth Elements via Solvent Extraction from a Neodymium Magnet Leachate and the Effects of Diluents. *Journal of Sustainable Metallurgy,* Volume 3, pp. 601-610.

Gregoric, M., Ravaux, C., Steenari, Espegren, F. & Retegan, T., 2018. Leaching and Recovery of Rare-Earth Elements from Neodymium Magnet Waste Using Organic Acids. *Metals.*

Gruber, V. & Carsky, M., 2020. New technology for lanthanide recovery from spent Nd-Fe-B magnets. *South African Journal of Chemical Engineering,* Volume 33, pp. 35-38.

Haque, N., Hughes, A., Lim, S. & Vernon, C., 2014. Rare Earth Elements: Overview of Mining, Mineralogy, Uses, Sustainability and Environmental Impact. *Resources,* Volume 3, pp. 614-635.

✓

Hidayah, N. & Abadin, S., 2018. The evolution of mineral processing in extraction of rare earth elements using liquid-liquid extractraction: A review. *Minerals Engineering,* Volume 121, pp. 146-157.

Hulanicki, A., Zurawaska, M. M. & Glab, S., 2005. Titrimetry: Potentiometric. In: P. Worsfold, C. Poole, A. Townshend & M. Miro, eds. *Encyclopedia of Analytical Science.* s.l.:Elsevier, pp. 121-128.

Massari, S. & Ruberti, M., 2012. Rare earth elements as critical raw materials: Focus on international markets and future strategies. *Resources Policy,* Volume 38, pp. 36-43.

Nagaphani, K. & Binnemans, K., 2018. Effect of the diluent on teh solvent extraction of neodymium by bis(2-ethylhexyl)phosphoric acid (D2EHPA). *Hydrometallurgy,* Volume 177, pp. 146-151.

Nakashima, K., Kubota, F., Maruyama, T. & Goto, M., 2005. Feasibility of Ionic Liquids as Alternative Separation Media for Industrial Solvent Extraction Processes. *Industrial & Engineering Chemistry Research,* 44(12), pp. 4368-4372.

Nascimento, M., Valverde, B. & Ferreira, F., 2015. Separation of rare earths by solvent extraction using DEHPA. *Metallurgy and materials,* 68(4), pp. 427-434.

Nayak, P.K., Kumaresan, R., Venkatesan, K.A., Antony, M.P. & Vasuveda Rao, P.R., 2014. Extraction Bheaviour of Am(III) and Eu(III) from Nitric Acid Medium in Tetraoctyldiglycomide-Bis(2-Ethylhexyl)Phospohoric Acid Solution. *Separation Science Technology,* 49(8), pp. 1186-1191.

NIST, 2019. *Combined Standard Uncertainty.* [Online] Available at: https://www.nist.gov/pml/nist-technical-note-1297/nist-tn-1297-5-combined-standard-uncertainty [Accessed 24 May 2021].

NIST, 2019. *Type A Evaluation of Standard Uncertainty.* [Online] Available at: 2021 [Accessed 24 May 2021].

NIST, 2019. *Type B Evaluation of Standard Uncertainty.* [Online] Available at: https://www.nist.gov/pml/nist-technical-note-1297/nist-tn-1297-4-type-b-evaluation-standard-uncertainty [Accessed 24 May 2021].

Peelman, S., Sun, Z., Sietsma, J. & Yang, Y., 2015. Leaching of Rare Earth Elements: Review of Past and Present Technologies. In: I. De Lima & W. Filho, eds. *Rare Earth Industry: Technological, Economic, and Environmental Implications.* s.l.:Elsevier, pp. 319 - 334.

PerkinElmer, 2018. *Sensitivity, Background, Noise, and Calibration in Atomic Spectroscopy: Effects on Accuracy and Detection Limits,* Waltham: PerkinElmer.

Prodius, D., Gandha, K., Mudring, A. V. & Nlebedim, I. C., 2019. *Sustainable Urban Mining of Critical Elements from Magnet and Electronic Wastes,* United States: ACS Publications.

Qi, D., 2018. Extractants Used in Solvent Extraction-Separation of Rare Earths: Extraction Mechanism, Properties, and Features. In: *Hydrometallurgy of Rare Earths: Extraction and Separation.* s.l.:Elsevier, pp. 187-389.

Roskill, 2016. *Rare earths: Global industry, markets and outlook,* London, UK: Roskill.

Rout, A., Venkatesan, K., Srinivasan, T. & Vasudeva Rao, P., 2011. Extraction and third phase formation behviour of Eu(III) in CMPO-TBP extractants present in room temperature ionic liquid. *Separation and Purification Technology,* Volume 76, pp. 238-243.

Santa Cruz Biotechnology, 2017. *Tributylmethylphosphonium methyl sulfate.* [Online] Available at: https://datasheets.scbt.com/sds/aghs/en/sc-237267.pdf [Accessed 5 May 2021].

Scholar Chemistry, 2009. *Material Safety Data Sheet: Iron(III) Oxide.* [Online] Available at: https://www.mccsd.net/cms/lib/NY02208580/Centricity/Shared/Material%20Safety%20Data%20Sheets%20_MSDS_/MSDS%20Sheets_Iron_III_Oxide_Red_378_00.pdf [Accessed 5 May 2021].

Seader, J., Henley, E. & Roper, D., 2011. Liquid-Liquid Extraction with Ternary Systems. In: *Separation Process Principles: Chemical and Biochemical Operations.* United States of America: John Wiley & Sons, Inc., p. 299.

Sigma-Aldrich , n.d. *Tributylmethylphosphonium methyl sulfate.* [Online] Available at: https://www.sigmaaldrich.com/catalog/product/aldrich/94456?lang=en&region=ZA [Accessed 10 May 2021].

Sigma-Aldrich, 2018. *Safety Data Sheet: Neodymium(III) Oxide.* [Online]✓ Available at: https://www.sigmaaldrich.com/MSDS/MSDS/DisplayMSDSPage.do?country=ZA&language=en&productNumber=203858&brand=ALDRICH&PageToGoToURL=https%3A%2F%2Fw

ww.sigmaaldrich.com%2Fcatalog%2Fproduct%2Faldrich%2F203858%3Flang%3Den [Accessed 5 May 2021].

Sigma-Aldrich, 2019. *Safety Datasheet: Bis(2-ethylhexyl) phosphate.* [Online] Available at: https://www.sigmaaldrich.com/MSDS/MSDS/DisplayMSDSPage.do?country=ZA&language =en&productNumber=237825&brand=ALDRICH&PageToGoToURL=https%3A%2F%2Fw ww.sigmaaldrich.com%2Fcatalog%2Fproduct%2Faldrich%2F237825%3Flang%3Den [Accessed 5 May 2021].

Sun, A., Luo, H. & Dai, S., 2012. Solvent extraction of rare-earth ions based on functionalised ionic liquids. *Talanta,* Volume 90, pp. 132-137.

ThermoFisher Scientific, 2019. *Safety Data Sheet: Nitric Acid.* [Online] Available at: https://www.fishersci.com/msds?productName=A467250%26productDescription=NITRIC [Accessed 5 May 2021].

Trilab Support Balance and Scale Service, 2021. *On-site Mass Calibration Certificate.* Durban, South Africa: s.n.

Tunsu, C., Menard, Y., Eriksen, D.O., Ekberg, C. & Petranikova, M., 2019. Recovery of critical materials from mine tailings: A comparitive study of the solvent extraction of rare earths using acidic, solvating and mixed extractant systems. *Journal of Cleaner Production,* Volume 218, pp. 425-437.

T unsu, C., Petranikova, M., Gregoric, M., Ekberg, C. & Retegan, T., 2015. Reclaiming rare earth elements from end-of-life products: A review of the perspectives for the urban mining using hydrometallurgical unit operations. *Hydrometallurgy,* Volume 156, pp. 239-258.

Villemin, D. & Didi, M., 2013. Extraction of Rare Earth and Heavy Metals, Using Ionic Solvents as Extraction Medium (A Review). *Oriental Journal of Chemistry,* 29(4), pp. 1267-1284.

Wang, M., Tan, Q., Chiang, J. & Li, J., 2017. Recovery of rare and precious metals from urban mines - A review. *Frontiers of Environmental Science & Engineering* .

Xie, F., Zhang, T., Dreisinger, D. & Doyle, F., 2014. A critical review of solvent extraction of rare earths from aqueous solutions. *Minerals Engineering,* Volume 56, pp. 10-28.

Appendix A: Memorandum of Understanding

such techniques, and what kind of equipment is available. The supervisor should also give guidance as to how information should be collected and later, in the writing up of the report, how results are analysed and presented in a scholarly way.

Field trips that are essential for the project are to be arranged by the supervisor.

The supervisor has to submit a Supervisor's report on the student's progress and contribution to the project. This must be submitted by the due date of the final laboratory project report.

Should the project require ethical clearance from the university or any other kind of permit (for example for collecting indigenous plants), then it is the supervisor's responsibility to obtain these. However, the student has to assist in preparing the necessary documentation.

The supervisor/technician has to bring the relevant safety rules to the student's attention and it is the responsibility of the student to abide by the rules of the discipline, School and University in terms of code of conduct and, health and safety regulations.

The supervisor should also clarify co-authorship of papers with the student and co-supervisors.

D)   Final report

Students are advised to write up their results as their research progresses, typically in the form of chapters of the final report. The supervisor will advise on how to go about the writing-up. The supervisor will read chapters handed in by the student and give feedback within a reasonable time, if such an agreement is made. It is, however, not the supervisor's job to proofread chapters.

The decision on the format of the report is made by the supervisor in consultation with the student.

The university rules for plagiarism apply.

Should parts of the report be published, then the supervisor in consultation with the student will decide which authors appear on the paper, and in which order. In this decision, the supervisor will take into account the contributions of the co-supervisor, student, and possibly third parties, to the part of the project that is to be published. A supervisor may publish results obtained by a undergraduate student without consulting the student if within one year of submission of the report no attempt has been made by the student to publish the results or to extend the research leading to these results.

If the student is bound by a confidentiality agreement, for example with a sponsor, then it is the student's and Supervisor's responsibility to make sure that the agreement is honoured.

Legal opinion must be sought regarding the matter of intellectual property, particularly in terms of Supervisors who are funded by external Organisations but have a student needing to withdraw.

E)   Running and Travel Expenses

Should the project require use of expensive chemicals, samples, or equipment, costs of fieldtrips, travel and any other expenses, all this must be specified on a separate sheet and presented to the Academic Leader. Such expenses must be discussed and payment confirmed; responsibility for these expenses made clear before the presentation of topics to the students. The discipline/cluster operates on a strict allowance per project and any additional expenses must be covered by the supervisor.

F)   Collegiality

Student and supervisor should treat each other with respect and dignity. In the interest of the research project, student and supervisor should keep each other informed about any activity relating to or relevant for the project. It is unacceptable for either party to submit results of the research project for publication or to present

2

them at a conference without prior consultation with the other party.

G)   Time Frames

Student and supervisor should agree on time frames for different phases of the project, these time frames should be reviewed at least annually.

H)   Conflict Resolution

Should there be a conflict or disagreement between supervisor and student which cannot be resolved by the parties involved, then either party can approach the Academic Leader of the Discipline or Dean and Head of School about the conflict. The Academic Leader of the Discipline or Dean and Head of School will then either arbitrate or choose a senior academic of the School not involved in the conflict to arbitrate. The arbitrator's decision is final and cannot be appealed.

Signatures:

Student ....Riyantha Moodley:................ Sohana Bridgemohan:........................

Date ...24/03/2021...

Supervisor......(*P Naidoo signs on behalf of all supervisors*)......

Date ......26-March-2021...

<u>**Note**</u>
Copies of this must be attached to your laboratory project proposal document.

Appendix B: Research Proposal & Gantt Chart

School of Engineering
University of KwaZulu-Natal
ENCH4LA Laboratory Project Proposal Template

Name of student: Riyantha Moodley   **Student no.** 218009136
Name of student: Sohana Bridgemohan   **Student no.** 218010264

Topic 22: Urban Mining of Rare Earth Elements from Rare Earth Magnets – Alternate Solvents for Extraction

Supervisor/s: Prof P Naidoo, Dr Williams-Wynn and Dr K Moodley

a) Problem Identification:

Iron (Fe) and boron (B) exist in a leaching solution with neodymium (Nd), a rare earth element (REE). The inability of sending waste electrical and electronic (WEEE) materials to landfills has increased research into recovery of REE's from WEEE to promote recycling. However, there lacks data in literature reporting on the separation of Fe from an aqueous HNO_3 solution via an HDEHP-based solvent, in the context of Nd recovery from waste NdFeB magnets. As such, this research study investigates the effect of the aforementioned extent of Fe separation as well as whether the separation is improved by ionic liquid doping.

b) Rationale and Motivation:

Rare earth metals (REM's), a group of 17 chemical elements, are important in today's society due to their properties that have enabled their contribution into many areas of technological advancements (Gergoric, et al., 2017). With the high demand for electronic and electrical equipment, it has been established that the REM's are crucial components in the manufacturing of the aforementioned devices. Nd has a wide variety of uses: the manufacturing of powerful magnets and computer hard drives. Nd magnets (NdFeB) are crucial components required in the production of wind turbines and hybrid cars; given the global shift in interest towards these green technologies, there is a high demand for these NdFeB magnets. Thus, the focus of this research proposal is neodymium, particularly NdFeB magnets.

Recycling of REM's found in WEEE is a prominent topic of interest. Scarcity of economically viable REM deposits with concerns of insufficient energy resources compromises run-of-mine extraction. Thus, there exists a need for REM recovery from secondary sources. Additionally, the pending ban of WEEE from landfills in South Africa creates an urgency for the development of a suitable technology for REM extraction. The recycling of e-wastes has the following advantages: alleviating the shortage, energy savings in mining and processing; resource conservation and reduction in pollution and greenhouse emissions.

According to (Prodius, et al., 2019), recycling of REM's via chemical recovery methods involves either pyrometallurgical or hydrometallurgical approaches. Hydrometallurgical processing of WEEE materials is considered a traditional approach to extract REM's. It is preferred over pyrometallurgical approaches since large amounts of solid wastes are generated and the process can be quite energy-consuming. Additionally, hydrometallurgical processing enables higher recovery rates of REM's.

Consequently, this research study focuses on hydrometallurgical processing. It involves comminution of waste material, leaching of the chemical constituents and separation of the individual elements via solvent extraction (Wang, et al., 2017). Solvent extraction is the separation of the constituent target REE by contact of a liquid with an insoluble organic solution (Ashiq, et al., 2019).

Due to the lack of availability of existing solvent extraction data of Nd, Fe, B (within the aqueous-organic system of interest) respectively, there exists a need to experimentally measure the extraction of each of these components within this system. The extraction data of these individual components in solution is necessary to enable future studies into the extraction from a real leachate solution containing all 3 elements. Ultimately, this would form the basis of future developments of a potentially commercial hydrometallurgical process for the beneficiation of NdFeB magnets.

This research project contributes towards the aforementioned future work, by generating the solvent extraction data of Fe. Nayak, et al. (2014) reported on the equivalent exchange of hydrogen ions from HDEHP with Am(III) ions in nitric acid; thus, it is expected that Fe^{3+} ions bound to nitrate ions in the aqueous phase will be absorbed into the organic phase through a similar mechanism.

c) Research Aims & Objectives:

The aim of this research project is to investigate the degree of extraction of Fe^{3+} ions from an aqueous nitric acid solution, contacted with an organic solvent (bis(2-ethylhexyl) phosphate, "HDEHP", diluted with n-dodecane), via an existing bench-scale, batch LLE set up. This aim will be met through the execution of the following objectives:

i. Verify the existing experimental method by performing experiments with Nd.
ii. Measurement of the distribution ratio of Fe^{3+} ions with varying nitric acid concentrations at 25°C, to establish the optimal aqueous acid concentration for Fe^{3+} recovery, using the above-mentioned organic solvent.
iii. Measurement of the distribution ratios of Fe^{3+} ions with the above-mentioned organic solvent that is doped with an ionic liquid (tributylmethylphosphonium methyl sulfate) at varying concentrations (0.01M, 0.1M and 0.25M, respectively).
iv. Infer the feasibility of this separation method as a pilot- or commercial-scale process based on analysis of the results.

d) Work plan – Research Activities:

Activity	Purpose	Timeframe
Literature Review	Report existing theory regarding the REE recovery, solvent selection and known extraction mechanisms	Ongoing (08/03/2021 – 18/05/2021)
Experimental Work: Test system (Nd_2O_3 extraction) New system (Fe_2O_3 extraction) Repeat new system with ionic liquid Analysis (ICP-OES)	Collect experimental data to: Verify experimental method, obtain new data (with and without ionic liquid) and determine distribution coefficients of Fe^{3+}	4- 5 weeks (Based on laboratory schedule)
Oral presentation of research project	Critical assessment	1 day (04/05/2021)
Submission of research project report	Critical assessment to present findings and display results and conclusions	Work will be ongoing Submission = 1day (18/05/2021)

e) Resources:

The following equipment will be used:
- LLE apparatus (Thermodynamics Research Unit)
- Mass balance (TRU)
- Wet chemistry glassware (titrations for pH determination) (TRU)
- ICP-OES Spectrophotometer (PMB Chemistry)
- Sample containers and vials

In addition, the following chemicals will be utilized:

- Nitric acid, Nd_2O_3, Fe_2O_3 powder, HDEHP, n-dodecane and ionic liquid (tributylmethylphosphonium methyl sulphate)

f) References

Ashiq, A., Kulkarni, J. & Vithanage, M., 2019. *Hydrometallurgical Recovery of Metals From E-waste,* Sri Lanka: Elsevier Inc.

Gergoric, M.; Ekberg, C.; Foreman, M.R.S.J.; Steenari1, B.M. & Retegan, T., 2017. *Characterization and Leaching of Neodymium Magnet Waste and Solvent Extraction of the Rare-Earth Elements Using TODGA,* Europe : Springer.

Nayak, P.K.; Kumaresan, R.; Venkatesan, K.A.; Antony, M.P.; Vasuveda Rao, P.R. 2014. Extraction Bheaviour of Am(III) and Eu(III) from Nitric Acid Medium in Tetraoctyldiglycomide-Bis(2-Ethylhexyl)Phospohoric Acid Solution. *Separation Science Technology,* 49(8), pp. 1186-1191.

Prodius, D., Gandha, K., Mudring, A. V. & Nlebedim, I. C., 2019. *Sustainable Urban Mining of Critical Elements from Magnet and Electronic Wastes,* United States: ACS Publications.

Wang, M., Tan, Q., Chiang, J. & Li, J.F., 2017. Recovery of rare and precious metals from urban mines - A review. *Frontiers of Environmental Science & Engineering,* 11(5), pp. 1-17.

Safety evaluation

Hazards – Equipment:

Exercise caution when working with the experimental apparatus to ensure no water comes into contact with any electrical cables or power sockets.

Hazards – chemicals:

- Nitric acid: Causes severe skin burns (requires nitrile gloves and proper storage) and eye damage, acute inhalation toxicity (mists), requires inhalation protection.
- Fe_2O_3: Use with adequate ventilation.
- HDEHP: Mildly flammable and toxic; harmful in contact with the skin; inhalation may cause irritation of lungs/throat, use in a well-ventilated area, with respirator.
- n-Dodecane: Flammable and inhalation hazard, requires respiration protection.
- Nd_2O_3: Handle with nitrile gloves
- Tributylmethylphosphonium methyl sulphate: Do not inhale fumes (acute oral toxicity).

PPE: Lab coat, safety mask (A-P Filter), tight-sealing safety goggles, protective gloves (nitrile) and safety shoes.

We, the students have read the MSDS for all chemicals to be used, and are aware of the health and safety rules when working in the laboratories.

Yes ☒   No ☐

Note: Any student/s caught in contravention of the health and safety rules of the School will face disciplinary action.

Signature of candidates: *[signatures]*   **Date: 24/03/2021**

I (we), …Paramespri Naidoo, the supervisor(s) of the student project have checked all possible hazards from the equipment, procedures and materials used in the project, and have instructed the students about safe working practice. *[This will be done once the students are allowed in the laboratory; students have been through the equipment via a video call with the MSc.Eng. student, Thulani Bayeni]*

Signature of Main Supervisor: **25 March 2021**

TOPIC 22: GANTT CHART

PROJECT MEMBERS: RIYANTHA MOODLEY (218009136)
SOHANA BRIDGEMOHAN (218010264)

SUPERVISORS: Prof P Naidoo
Dr M Williams-Wyn
Dr K Moodley

	START DATE	END DATE
	8/3/2021	18/5/2021

Task ID	Task Name	Start Week	End Week	WK01	WK02	WK03	WK04	WK05	WK06	WK07	WK08	WK09	WK10	WK11	WK12
1	Deliverable: Safety forms	WK01	WK01	■											
2	Deliverable: Research proposal and MOU	WK01	WK02	■	■										
3	Deliverable: Gantt chart	WK01	WK02	■	■										
4	Literature review	WK01	WK12	■	■	■								■	■
5	Progress assessment with supervisor	WK01	WK12	■	■	■								■	■
6	Experimental work	WK03	WK03			■									
6.1	Perform a test run (Neodymium extraction)	WK03	WK03			■									
6.2	Solvent extraction measurements	WK04	WK05				■	■							
6.3	Solvent extraction measurements (with IL doping)	WK05	WK06					■	■						
6.4	ICP-OES sample analysis (PMB Chemistry)	WK07	WK07							■					
6.5	Analysis & discussion of results	WK07	WK12							■	■	■	■	■	■
7	Presentation	WK03	WK09			■	■	■	■	■	■	■			
7.1	Presentation preparation	WK03	WK09			■	■	■	■	■	■	■			
7.2	Presentation slides	WK07	WK09							■	■	■			
7.3	Deliverable: Presentation	WK09	WK09									■			
8	Final report	WK01	WK12	■	■	■	■	■	■	■	■	■	■	■	■
8.1	Final report writing	WK01	WK12	■	■	■	■	■	■	■	■	■	■	■	■
8.2	Deliverable: Final report	WK12	WK12												■

Appendix C: Raw Data

C.1: Solution Synthesis - Measured

- The measured quantities of each component used to make the aqueous and organic phases are, for all three experimental runs, are presented in Table C-1. Values are reported as presented on the analytical balance (readability 0.00001g)

Table C-1: Measured Quantities – Solution Synthesis

Species	Experimental Run (i)			Experimental Run (ii)			Experimental Run (iii)		
Aqueous Phase									
Desired $[HNO_3]$	0.1M	0.5M	0.9M	0.1M	0.5M	0.9M	0.1M	0.5M	0.9M
Flask [g]	53.8096	53.2889	55.9431	52.8060	53.8426	83.3130	53.1786	56.4324	51.8778
Nd_2O_3 [g]	0.0544	0.0511	0.05040	N/A	N/A	N/A	0.0221	0.0210	0.0221
Fe_2O_3 [g]	N/A	N/A	N/A	0.0713	0.0766	0.0703	0.0506	0.0493	0.049
HNO_3 [g]	0.2638	1.0429	1.8320	0.4620	1.5846	2.6730	0.446	1.5343	2.615
H_2O [g]	24.5561	23.9769	23.6932	34.3286	33.5004	32.6970	34.3425	33.5656	32.7648
Organic Phase									
Flask [g]	52.8380						53.2969		
HDEHP [g]	14.5867						7.2605		
n-Dodecane[g]	56.3005						28.1412		

C.2: LLE Samples

The masses of the organic and aqueous phases were recorded, respectively, for a pipetted volume of 5 mL into the test compartments, as indicated in Table C-2. The letter next to each vial number indicates the student responsible for the dispensing, sampling and analysis of that vial's contents. The designation is as follows: R – Riyantha Moodley (218009136), S – Sohana Bridgemohan (218010264). These masses were required when evaluating the uncertainty of measurement in the analytical mass balance.

Table C-2: Measured Values – Vial Preparation

Vial # (R/S)	[HNO$_3$] [M]	Vial Mass [g]	Aqueous Mass [g]	Organic Phase [g]
Nd Test System				
1 – R	0.1M	18.7694	4.5868	3.6230
2 – R	0.5M	18.1404	4.6264	3.6356
3 – R	0.9M	18.1839	4.6730	3.6322
4 – S	0.1M	17.2695	4.6169	3.6039
5 – S	0.5M	18.6380	4.6302	3.5860
6 – S	0.9M	17.9431	4.6173	3.6341
Fe (no IL)				
1 – R	0.1M	18.7252	4.5937	3.6510
2 – R	0.5M	18.1403	4.6468	3.6569
3 – R	0.9M	18.1829	4.6973	3.6723
4 – S	0.1M	17.2691	4.6304	3.629
5 – S	0.5M	18.5989	4.6090	3.6208
6 – S	0.9M	17.9429	4.6717	3.6105
Fe (with IL)				
1 – R	0.1M	18.8123	4.5947	3.6782
2 – R	0.5M	18.1380	4.7144	3.5852
3 – R	0.9M	18.1813	4.7409	3.5747
4 – S	0.1M	17.7148	4.6066	3.6081
5 – S	0.5M	18.7015	4.6659	3.6335
6 – S	0.9M	17.6408	4.676	3.6178

C.3: ICP-OES Results

The ICP-OES results were as per analysis at the Department of Chemistry (PMB campus). The reported aqueous phase metal loading post extraction is presented in Figures C-1 and C-2, with reference to the corresponding ICP calibration standard that was prepared. Note that samples denoted with "R" or "S" are relevant to this investigation.

UNIVERSITY OF
KWAZULU-NATAL ™
INYUVESI
YAKWAZULU-NATALI

UKZN PMB CHEMISTRY LAB
ICP RESULTS
DATE: 20 April 2021

To: Dr Mark Williams-Wynn
Thermodynamics Research Unit
School of Engineering
UKZN

Sample Labels	Nd 401.224	Nd 406.108	Nd 410.945
0,5N2,9B	20,1	20,1	20,1
0,5N 0,1C	2,01	2,03	2,02
0,5N 0,9C	17,7	17,7	17,7
0,5N2,9C	20,6	20,7	20,7
0,1N 0,1A	8,6	8,6	8,6
0,1N 0,5A	20,1	20,2	20,1
0,1N 0,9A	17,9	18,0	17,9
0,1N 1,3A	19,4	19,5	19,5
0,1N 1,7A	19,7	19,8	19,7
0,1N 2,1A	19,9	20,0	20,0
0,1N 2,5A	20,9	21,1	21,0
0,1N 2,9A	20,5	20,6	20,5
0,1N 0,1B	9,02	9,10	9,03
0,1N 0,5B	20,6	20,8	20,6
0,1N 0,9B	20,7	20,9	20,8
0,1N 1,3B	20,3	20,5	20,3
0,1N 1,7B	20,4	20,6	20,4
0,1N 2,1B	20,2	20,5	20,2
0,1N 2,5B	20,2	20,5	20,2
0,1N 2,9B	20,8	21,0	20,8
0,1N 0,1C	8,77	8,87	8,76
0,1N 0,5C	20,0	20,3	20,0
0,1N 0,9C	20,4	20,7	20,3
0,1N 1,3C	20,1	20,4	20,0
0,1N 2,1C	18,5	18,8	18,5
0,1N 2,5C	19,7	20,1	19,8
0,1N 2,9C	20,8	21,2	20,8
0,01Q 0,1A	2,02	2,05	2,04
0,01Q 0,5A	12,6	12,8	12,6
0,01Q 0,9A	17,6	17,9	17,6
0,01Q 1,3A	19,5	19,9	19,4
0,01Q 1,7A	18,4	18,8	18,4
0,01Q 2,1A	19,9	20,3	19,9
0,01Q 2,5A	19,0	19,4	19,0
0,01Q 2,9A	19,9	20,4	19,9
0,01Q 0,1B	2,05	2,08	2,06
0,01Q 0,5B	12,5	12,6	12,5
0,01Q 0,9B	18,2	18,6	18,2
0,01Q 1,3B	19,0	19,4	19,0
0,01Q 1,7B	19,4	19,8	19,4
0,01Q 2,1B	20,7	21,1	20,7
0,01Q 2,5B	19,0	19,4	19,0
0,01Q 2,9B	20,2	20,6	20,1
0,01Q 0,1C	1,97	1,98	1,97
0,01Q 0,5C	12,1	12,2	12,1
0,01Q 0,9C	18,3	18,8	18,4
0,01Q 1,3C	18,8	19,2	18,9
0,01Q 1,7C	20,1	20,6	20,2
0,01Q 2,5C	19,4	19,9	19,5
0,01Q 2,9C	19,4	19,9	19,4
1N 0,1A	2,24	2,26	2,26
1N 2,9A	19,6	20,2	19,7
1N 0,1B	2,6	2,6	2,6
1N 2,9B	19,7	20,1	19,7
1N 0,1C	1,88	1,90	1,89
1N 2,9C	29,2	29,9	29,3
V1NR	2,03	2,06	2,05
V2NR	13,0	13,2	12,9
V3NR	18,7	19,2	18,7
V4NR	1,86	1,88	1,85
V5NR	4,09	4,10	4,09
V6NR	9,59	9,60	9,61

NOTE: Results are in mg/L
uv means under value

For queries concerning these results, please contact Ms Zimbini Ngcingwana, +27(0)33 260 5905
ngcingwanan@ukzn.ac.za

Figure C-1: Reported ICP-OES results – Run 1(Nd) (UKZN PMB, Chemistry Lab)

UNIVERSITY OF KWAZULU-NATAL ™
INYUVESI YAKWAZULU-NATALI

UKZN PMB CHEMISTRY LAB	To: Prof P. Prathieka Naidoo
ICP RESULTS	Dept of Chemical Engineering
DATE: 18 May 2021	School of Engineering
	UKZN

Sample Labels	Fe 259.940	Nd 401.224	Nd 406.108	Nd 410.945
V1FR	0,9532	-0.094770 uv	-0.086871 uv	-0.088454 uv
V2FR	0,9560	-0.030943 uv	-0.015643 uv	0,0044
V3FR	0,9562	0,0065	0,0184	0,1735
V4FS	0,9523	-0.100014 uv	-0.087680 uv	-0.069897 uv
V5FS	0,9541	0,2578	0,2820	0,3315
V6FS	1,23	0,0444	0,0677	0,1097
V1FLR	0,9673	-0.080671 uv	-0.063877 uv	0,0090
V2FLR	0,9545	-0.005244 uv	0,0197	0,0218
V3FLR	1,11	-0.028278 uv	-0.010218 uv	0,026376
V4FLS	1,03	-0.091125 uv	-0.080984 uv	-0.075839 uv
V5FLS	1,01	-0.092695 uv	-0.086981 uv	0,800392
V6FLS	1,03	-0.043805 uv	-0.033964 uv	0.001525 uv
V1NFR	0,9553	-0.015844 uv	-0.006959 uv	0,0068
V2NFR	0,9538	2,51	2,63	2,59
V3NFR	0,9536	3,78	3,93	3,72
V4NFS	0,9526	-0.086957 uv	-0.081597 uv	-0.044305 uv
V5NFS	0,9548	2,54	2,65	2,55
V6NFS	0,9544	3,76	3,90	3,76

NOTE: Results are in mg/L
uv means under value

For queries concerning these results, please contact Ms Zimbini Ngcingwana, +27(0)33 260 5905
ngcingwanan@ukzn.ac.za

Figure C-2: Reported ICP-OES results – Run 2(Fe) and Run 4 (Nd &Fe) (UKZN PMB, Chemistry Lab)

Note that the reported neodymium concentrations for the second experimental run may be ignored, as this was not intended to be measured.

C.4: Titration Measurements

Each student performed three measurements over the nitric acid concentration range. Each measurement was duplicated for the titration analysis, hence a total of 12 titration samples were analysed per experimental run, and are reported in Table C-3, C-4 and C-5. A NaOH titrant of concentration 0.029615 M was used during the analyses. The reported volume delivered and corresponding equilibrium acid concentration that was calculated is presented. The reported masses were required when evaluating the uncertainty of measurement in the analytical mass balance.

Table C-3 Titration Analysis Measurements – Run 1

Vial # (R/S)	Estimate [HNO$_3$]	Tube mass [g]	Tube & sample mass [g]	Estimate sample volume [mL]	Volume NaOH delivered [mL]	Calculated LLE [HNO$_3$] [M]	Average [HNO$_3$] [M]
1 – R	0.001M	12.6340	39.0412	26	0.6132	0.0699	0.08277
		12.5446	37.5779	25	0.8079	0.0957	
2 – R	0.005M	12.6424	38.2957	25.5	3.2454	0.377	0.3836
		12.5908	36.9043	24	3.1632	0.390	
3 – R	0.009M	12.6649	38.2483	25.5	5.2991	0.615	0.6110
		12.5563	37.7496	25	5.1211	0.607	
4 – S	0.001M	12.7286	37.9871	25	0.5736	0.0680	0.07774
		12.5320	38.2830	26	0.7685	0.0875	
5 – S	0.005M	12.7539	39.1811	26	2.5044	0.285	0.2517
		12.7271	37.9006	25	1.8419	0.218	
6 – S	0.009M	12.5753	39.0127	26	3.2059	0.365	0.3670
		12.7914	38.5656	25.5	3.1756	0.369	

Table C-4: Titration Analysis Measurements – Run 2

Vial # (R/S)	Estimate [HNO$_3$]	Tube mass [g]	Tube & sample mass [g]	Estimate sample volume [mL]	Volume NaOH delivered [mL]	Calculated LLE [HNO$_3$] [M]	Average [HNO$_3$] [M]
1 – R	0.001M	12.8218	37.8851	25	0.6978	0.08267	0.07266
		12.8322	36.4126	24	0.5078	0.06266	
2 – R	0.005M	12.7238	38.4341	26	3.3590	0.3826	0.3978
		12.6663	38.4121	26	3.6261	0.4130	
3 – R	0.009M	12.7536	37.1871	24	5.7397	0.7083	0.7098
		12.9627	38.0802	25	6.0055	0.7114	
4 – S	0.001M	12.7518	39.3457	27	1.3674	0.1500	0.1447
		12.4059	37.7289	25	1.1764	0.1394	
5 – S	0.005M	12.5633	37.5041	25	3.4018	0.4030	0.3959
		12.5565	38.0670	26	3.4129	0.3887	
6 – S	0.009M	12.3778	39.4278	27	3.2059	0.3516	0.3567
		12.5608	38.5383	26	3.1756	0.3617	

Table C-5: Titration Analysis Measurements – Run 4

Vial # (R/S)	Estimate [HNO$_3$]	Tube mass [g]	Tube & sample mass [g]	Estimate sample volume [mL]	Volume NaOH delivered [mL]	Calculated LLE [HNO$_3$] [M]	Average [HNO$_3$] [M]
1 – R	0.001M	12.9595	38.0594	25	0.9168	0.1086	0.1310
		12.8515	37.3866	25	1.2952	0.1534	
2 – R	0.005M	12.8576	38.775	26	3.4392	0.3917	0.3921
		12.8238	37.8293	25	3.3123	0.3924	
3 – R	0.009M	12.4724	37.0507	25	5.1625	0.6116	0.6299
		12.7616	37.4296	25	5.4718	0.6482	
4 – S	0.001M	12.7076	37.2274	25	1.0423	0.1235	0.1136
		12.899	37.1593	24	0.8409	0.1038	
5 – S	0.005M	12.7115	38.7582	26	3.2294	0.3678	0.3802
		12.7781	37.9497	25	3.3147	0.3927	
6 – S	0.009M	12.7577	36.9072	24	5.2987	0.6538	0.6548
		12.6548	37.8766	25	5.5363	0.6558	

C.5: Reported ICP-OES Calibrations

The ICP instrumentation was calibrated with the relevant standard for each experimental run. Note that neodymium ICP standards prepared during the post-graduate study were used for the test system. The calibration results, reported calibration curve and calculated RMSE are presented in Tables C-6 to C-13.

Table C-6: ICP-OES Reported Calibration – Run 1 (Nd 401.224)

Standard	Intensity [c/s]	Standard Concentration [mg/L]	Calculated Concentration [mg/L]	Error [mg/L]
Blank	245.4	0	1.719	-1.719
1	10881.5	2.91	3.603	-0.693
2	12444.7	4.85	3.880	0.970
3	21649.1	6.79	5.510	1.280
4	37611.6	9.7	8.337	1.363
5	106598.8	19.4	20.555	-1.155
6	264641.2	48.5	48.545	-0.045
Curve Type: Linear [a]		Correlation Coefficient = 0.997283		RMSE = 1.147

[a] Curve coefficient 1 = -9463.1, Curve coefficient 2 = 5646.38, Blank offset = -9463.1

Table C-7: ICP-OES Reported Calibration – Run 1 (Nd 406.108)

Standard	Intensity [c/s]	Standard Concentration [mg/L]	Calculated Concentration [mg/L]	Error [mg/L]
Blank	109.9	0	1.822	1.822
1	11122.2	2.91	3.598	-0.688
2	13020	4.85	3.904	0.946
3	22841.7	6.79	5.487	1.303
4	39783.6	9.7	8.219	1.481
5	116240	19.4	20.547	-1.147
6	290053.9	48.5	48.573	-0.073
Curve Type: Linear [a]		Correlation Coefficient = 0.99708		RMSE = 1.189

[a] Curve coefficient 1 = -11190.1, Curve coefficient 2 = 6201.87, Blank offset = -11190.1

52

Table C-8: ICP-OES Reported Calibration – Run 1 (Nd 410.945)

Standard	Intensity [c/s]	Standard Concentration [mg/L]	Calculated Concentration [mg/L]	Error [mg/L]
Blank	146.1	0	1.730	-1.730
1	12153	2.91	3.613	-0.703
2	14031.5	4.85	3.908	0.942
3	24416.4	6.79	5.536	1.254
4	41942.5	9.7	8.284	1.416
5	119946.3	19.4	20.514	-1.114
6	298854.1	48.5	48.565	-0.065
Curve Type: Linear [a]		Correlation Coefficient = 0.997285		RMSE =1.146

[a] Curve coefficient 1 = -10890.6, Curve coefficient 2 = 6377.906, Blank offset = -10890.6

Table C-9: ICP-OES Reported Calibration – Run 2 (Fe 259.940)

Standard	Intensity [c/s]	Standard Concentration [mg/L]	Calculated Concentration [mg/L]	Error [mg/L]
Blank	631.1	0	1.062	-1.062
1	1827.1	1	1.267	-0.267
2	9971.8	3	2.662	0.338
3	19046.3	5	4.217	0.783
4	32928.5	7	6.595	0.405
5	45080.2	9	8.676	0.324
6	114224.8	20	20.521	-0.521
Curve Type: Linear [a]		Correlation Coefficient = 0.995555		RMSE =0.594

[a] Curve coefficient 1 = -5569.95, Curve coefficient 2 = 5837.768, Blank offset = -5570

Table C-10: ICP-OES Reported Calibration – Run 4 (Fe 259.940)

Standard	Intensity [c/s]	Standard Concentration [mg/L]	Calculated Concentration [mg/L]	Error [mg/L]
Blank	753.5	0	-1.396	1.396
1	117425.2	20	20.327	-0.327
2	275220	50	49.708	0.292
3	439941.4	80	80.378	-0.378
4	563551.2	100	103.393	-3.393
5	800927.8	150	147.591	2.409
Curve Type: Linear [a]		Correlation Coefficient = 0.999353		RMSE =1.807

[a] Curve coefficient 1 = -5569.95, Curve coefficient 2 = 5837.768, Blank offset = -5570

Table C-11: ICP-OES Reported Calibration – Run 4 (Nd 401.224)

Standard	Intensity [c/s]	Standard Concentration [mg/L]	Calculated Concentration [mg/L]	Error [mg/L]
Blank	303.4	0	-0.987	0.987
1	231571	50	48.696	1.304
2	388486.8	80	82.406	-2.406
3	480631.6	100	102.201	-2.201
4	692354.9	150	147.685	2.315
Curve Type: Linear [a]		Correlation Coefficient = 0.999255		RMSE =1.932

[a] Curve coefficient 1 = 4896.465, Curve coefficient 2 = 4654.909, Blank offset = 4896.5

Table C-12: ICP-OES Reported Calibration – Run 4 (Nd 406.108)

Standard	Intensity [c/s]	Standard Concentration [mg/L]	Calculated Concentration [mg/L]	Error [mg/L]
Blank	145.7	0	-0.202	0.202
1	248438.3	50	48.483	1.517
2	420913.5	80	82.303	-2.303
3	513293.6	100	100.417	-0.417
4	761062	150	149.000	1.000
Curve Type: Linear [a]		Correlation Coefficient = 0.999648		RMSE =1.328

[a] Curve coefficient 1 =1177.821, Curve coefficient 2 = 5099.905, Blank offset =1177.8

Table C-13: ICP-OES Reported Calibration – Run 4 (Nd 410.945)

Standard	Intensity [c/s]	Standard Concentration [mg/L]	Calculated Concentration [mg/L]	Error [mg/L]
Blank	286.5	0	-0.873	0.873
1	239410.5	50	48.637	1.363
2	401614	80	82.221	-2.221
3	498268.6	100	102.233	-2.233
4	718253	150	147.781	2.219
Curve Type: Linear [a]		Correlation Coefficient = 0.999303		RMSE =1.869

[a] Curve coefficient 1 =4501.221, Curve coefficient 2 = 4829.807, Blank offset =4501.2

Appendix D: Sample Calculations

D.1: Solution Synthesis – Calculated Quantities

The masses of all components required to produce the feedstock solutions are presented in Tables D-1, D-2 and D-3 lists the quantities to produce the ICP standard solutions via successive dilution of the aqueous feed.

Table D-1: Calculated Masses - Aqueous Feed Solutions

Experimental Run	[HNO_3], [M]	Nd_2O_3 [g]	Fe_2O_3 [g]	HNO_3 [g]	H_2O [g]
1	0.1	0.050	N/A	0.264	24.549
	0.5	0.050	N/A	1.041	23.974
	0.9	0.050	N/A	1.818	23.400
2 & 3	0.1	N/A	0.070	0.446	34.307
	0.5	N/A	0.070	1.534	33.503
	0.9	N/A	0.070	2.622	32.700
4	0.1	0.021	0.049	0.423	34.326
	0.5	0.021	0.049	1.511	33.522
	0.9	0.021	0.049	2.599	32.718

Table D-2: Calculated Masses – Organic Feed Solutions

Experimental Run	0.5M HDEHP [g]	0.1M IL1[a] [g]	0.1M IL2[b] [g]	n-Dodecane [g]
1 & 2	14.508	N/A	N/A	56.259 ✓
3 (IL1 [a])	7.254	1.478	N/A	27.050
3 (IL 2 [b])	7.254	N/A	1.748	26.910
4	7.254	N/A	N/A	28.129

[a] – Tributylmethylphosphonium methyl sulfate; [b] - Tributylmethylphosphonium tosylate

Table D-3: Calculated Volumes – ICP Standards

Desired C_1 [ppm REM][a]	100	80	50	20	9	7	5	3	1
Starting C_1 [ppm REM][a]	2000	100	100	100	100	100	100	100	100
Diluted V_2 [mL]	100	25	25	25	25	25	25	25	25
Required V_1 [mL]	5	20	12.5	5	2.25	1.75	1.25	0.75	0.25

[a] Note that ppm is equivalent to mg/L

<u>Sample Calculation: Feed Solutions</u>

These quantities were calculated based on the required concentrations needed for each aqueous and organic phase in the experimental run. A sample calculation for the aqueous phase of the neodymium test system (0.1 M HNO₃) is presented.

✓

Since this feed will only be used in Run 1, this translates to 2 samples of 5 mL volume each. Hence a total volume of 10 mL of 0.1 M HNO₃ feed was required. An excess of 15 mL was accounted for in the event of spillages as well as to synthesise the ICP calibration standards. Thus a total solution volume of 25 mL was the basis. The required metal loading was 2000ppm.

✓

$$Required\ Nd_2O_3\ mass = V \times C = 25\ mL \times 2000 \left(\frac{mg}{L}\right) = 0.05g\ Nd_2O_3$$

$$Corresponding\ volume = \frac{mass}{density} = \frac{0.05g}{7.42g/cm^3} = 0.006739\ cm^3 = 0.06739\ mL\ Nd_2O_3$$

$$\therefore mols\ Nd_2O_3 = purity \times \frac{mass}{molar\ mass} = 0.99 \left(\frac{0.05g}{336.48g/mol}\right) = 0.0001486\ mols\ Nd_2O_3$$

1 mol Nd₂O₃ : 2 mol Nd³⁺ according to Equation 2-1

Hence there exist 0.0002972 mols of Nd³⁺ in solution.

✓

The corresponding HNO₃ required to dissolve the rare earth oxide is thus calculated, in the stoichiometric ratios stipulated by Equation 2-1. 1 mol Nd₂O₃ : 6 mol H⁺ : 6 mol HNO₃

$$\therefore Required\ H^+ = 6 \times mols\ Nd_2O_3 = 6 \times 0.0001486 = 0.0008915\ mols\ H^+$$

$$\therefore Required\ HNO_3 = required\ H^+ = 0.0008915\ mols\ HNO_3$$

$$\therefore Required\ HNO_3(pure) = 0.0008915\ mol \times \frac{63.01g}{mol} = 0.0562gHNO_3$$

✓

Aqueous HNO₃ solution was available at a molar purity of 0.55. The density of water is 18.015 g/cm³ and that of pure nitric acid is 1.51 g/cm³. The reported solution density was 1.34 g/cm³

$$\therefore required\ HNO_3 solution\ mass = 0.0562 \left(\frac{(0.55 \times 63.01) + ((1-0.55) \times 18.015)}{0.55 \times 63.01}\right)$$

$$= 0.06931\ g\ HNO_3 solution$$

$$\therefore Required\ HNO_3 solution\ volume = \frac{mass}{volume} = \frac{0.06931g}{1.34g/cm^3} = 0.0517\ mL\ solution$$

This is the required quantity of HNO₃ to dissolve the metal oxide into solution. More HNO₃ is required to form the desired concentration of 0.1 M.

An initial guess of the required HNO_3 solution mass was used. The guess value was 0.5 g.

$$\therefore mols\ HNO_3 = \frac{0.5g}{1.34g/cm^3} = 0.0117\ mol\ HNO_3\ solution$$

$$\therefore mols\ of\ H^+ in\ solution = 0.55 \times 0.0117 = 0.006431\ mols\ H^+$$

$$\therefore H^+ concentration = \frac{mols\ H^+}{\frac{mass\ HNO_3}{density\ HNO_3}} = \frac{0.006431 mols}{\frac{0.5g}{1.34g/cm^3)}} = 17.235\ M$$

✓

The remaining HNO_3 in the aqueous feed after consuming the metal oxide is calculated by difference:

$$\therefore remaining\ H^+ after\ consumption = 0.006431 - 0.0008915 = 0.005539\ mols\ H^+$$

$$\therefore remaining\ H^+ concentration = \frac{mols\ H^+}{\frac{mass\ HNO_3}{density\ HNO_3}} = \frac{0.005539}{\frac{0.5g}{1.34g/cm^3}} = 14.8456\ M\ HNO_3 \quad ✓$$

$$volume\ HNO_3 = \frac{0.5g}{1.34g/cm^3} = 0.3731\ mL\ HNO_3\ solution$$

The desired HNO_3 concentration of the feed is 0.1 M. Thus, it needs to be diluted from 14.8456M to 0.1 M. Using the dilution formula $C_1V_1 = C_2V_2$:

$$Required\ diluent\ (water) = \frac{14.8456\ M \times 0.3731\ mL}{0.1\ M} - 0.3731\ mL = 55.02098\ mL\ water$$

$$\therefore Required\ diluent\ mass = \frac{55.02098\ mL}{0.99g/cm^3} = 54.471\ g\ water$$

Thus, the total masses and corresponding masses for each specie in the aqueous phase was determined:

$$\therefore Total\ feed\ mass = m_{Nd_2O_3} + m_{HNO_3} + m_{H_2O} = 0.05 + 0.5 + 54.471 = 55.021g$$

$$\therefore Total\ feed\ volume = V_{Nd_2O_3} + V_{HNO_3} + V_{H_2O} = 0.006739 + 0.3731 + 55.021$$

$$= 55.401\ mL$$

The total solution volume was then specified to be the required 25 mL using Microsoft Excel's Solver tool, by solving for the total HNO_3 mass required (the initial guess of 0.5g).The converged values are those presented in Table D-1. The metal oxide concentration was also found.

Note that to obtain the true feed concentration, the measured masses of each component was inserted into the above calculation. However, Solver was not required. Using the aforementioned values, the true concentration was calculated as follows:

$$True\ [HNO_3] = \frac{14.8456M \times 0.3731mL}{0.3731mL + 55.02098\ mL} = 0.2169\ M\ HNO_3$$

✓

<u>Sample Calculation: ICP Calibration Standards</u>

The aqueous feed (2000 ppm) was successively diluted to produce the ICP calibration standards at various concentrations. The first standard was at a concentration of 100 ppm, and a volume of 100 mL was to be prepared.

Denoting '1' as the starting solution (2000 ppm) and '2' as the solution to be prepared:

$$C_1 V_1 = C_2 V_2 \Rightarrow V_1 = \frac{C_2 V_2}{C_1}$$

$$\therefore V_1 = \frac{100 \ ppm \times 100 \ mL}{2000 \ ppm} = 5mL \ \text{of the 2000 ppm solution is required.}$$

D.2: Titration Analysis

The volume of NaOH (0.029615 M) delivered for each titration measurement is reported in Appendix C.4, for each experimental run. A sample calculation for the neodymium test system (run1) is presented for Vial 4 – S, the measurements for which are presented in Table C-3.

Sample 1:

Approximate sample volume = 25 mL (based on sample level in graduated centrifuge tube)

Approximate sample concentration = 0.001 M. Denoting '1'as the aqueous feed and '2' as the NaOH titrant:

$$C_1 V_1 = C_2 V_2 \Rightarrow C_1 = \frac{C_2 V_2}{V_1} = \frac{0.029615 \ M \times 0.5736 \ mL}{25 \ mL} = 0.0680 \ M \ HNO_3$$

Sample 2:

Approximate sample volume = 26 mL (based on sample level in graduated centrifuge tube)

Approximate sample concentration = 0.001 M. Using the aforementioned designation:

$$C_1 V_1 = C_2 V_2 \Rightarrow C_1 = \frac{C_2 V_2}{V_1} = \frac{0.029615 \ M \times 0.7685 \ mL}{26 \ mL} = 0.0875M \ HNO_3$$

Average HNO$_3$ concentration for Vial 4 – S:

$$Average \ concentration = \frac{0.0680 \ M + 0.0875 \ M}{2} = 0.07774 \ M \ HNO_3$$

D.3: Distribution Coefficients

The results used to calculate the distribution coefficient in each experimental run is presented in Tables D-4 to D-7.

Table D-4: Distribution Coefficient – Run 1

Vial (R/S)	True Feed [HNO$_3$], [M]	Feed [Nd] [mg/L]	Average ICP [Nd] (diluted) [mg/L]	Average ICP [Nd] [mg/L]	Organic Phase [Nd]	D$_{Nd}$
1-R	0.0969	2175.27	2.04667	204.667	1970.61	9.628
2-R	0.500	2043.65	13.0333	1303.33	740.62	0.568
3-R	0.896	1991.58	18.8667	1886.67	104.92	0.0556
4-S	0.0969	2175.27	1.8633	186.33	1988.94	10.674
5-S	0.500	2043.65	4.0933	409.33	1634.32	3.993
6-S	0.896	1991.58	9.6	960	1031.58	1.075

Table D-5: Distribution Coefficient – Run 2

Vial (R/S)	True Feed [HNO$_3$], [M]	Feed [Fe] [mg/L]	Average ICP [Fe] (diluted) [mg/L]	Average ICP [Fe] [mg/L]	Organic Phase [Fe]	D$_{Fe}$
1-R	0.105	2035.18	0.9532	95.32	1939.86	20.35
2-R	0.512	2186.33	0.9560	95.60	2090.73	21.87
3-R	0.918	2006.54	0.9562	95.62	1910.92	19.98
4-S	0.105	2035.18	0.9523	95.23	1939.95	20.37
5-S	0.512	2186.33	0.9541	95.41	2090.92	21.92
6-S	0.918	2006.54	1.23	123	1883.54	15.31

✓

Table D-6: Distribution Coefficient – Run 4 (Fe)

Vial (R/S)	True Feed [HNO₃], [M]	Feed [Fe] [mg/L]	Average ICP [Fe] (diluted) [mg/L]	Average ICP [Fe] [mg/L]	Organic Phase [Fe]	D_{Fe}
1-R	0.106	1444.28	0.9553	95.53	1348.75	14.12
2-R	0.507	1406.07	0.9538	95.38	1310.69	13.74
3-R	0.904	1397.62	0.9536	95.36	1302.26	13.66
4-S	0.106	1444.28	0.9526	95.26	1349.02	14.16
5-S	0.507	1406.07	0.9548	95.48	1310.59	13.73
6-S	0.904	1397.62	0.9544	95.44	1302.18	13.64

Table D-7: Distribution Coefficient – Run 4 (Nd)

Vial (R/S)	True Feed [HNO₃], [M]	Feed [Nd] [mg/L]	Average ICP [Nd] (diluted) [mg/L]	Average ICP [Nd] [mg/L]	Organic Phase [Nd]	D_{Nd}
1-R	0.106	630.80	0.009868	0.9868	629.81	638.26
2-R	0.507	598.94	2.5767	257.67	641.27	1.32
3-R	0.904	630.36	3.8100	381.00	249.36	0.65
4-S	0.106	630.80	u/v	u/v	N/A	N/A
5-S	0.507	598.94	2.5800	258.00	340.94	1.32
6-S	0.904	630.36	3.8067	380.67	249.69	0.66

A sample calculation is presented for the distribution ratio of Vial 4 (S) of the neodymium test system (run 1, Table D-4).

The method to determine true feed concentration of nitric acid and neodymium is as described in Appendix D1. The average post-extraction neodymium concentration is obtained by taking an average of the3 ICP results reported for each corresponding calibration standard, as reported in Figure C-1

$$\therefore Average \ [Nd]_{aqueous} = \frac{1.86+1.88+1.85}{3} = 1.8633 \ mg/L$$

Note that the aqueous phase (after extraction) was diluted in the ratio of 1:100 to produce the sample for analysis. Hence, the true metal ion concentration in the aqueous phase is:

$$\therefore [Nd^{3+}]_{aqueous} = 100 \times 1.8633 = 186.33 \ mg/L$$

The concentration of neodymium in the aqueous phase prior to extraction was found to be 2175.27 mg/L. Thus the concentration of neodymium in the organic phase is found be difference:

$$[Nd]_{organic} = [Nd]_{aqueous, \ before} - [Nd]_{aqueous, \ after}$$
$$[Nd]_{organic} = 2175.27 - 186.33 = 1988.94$$

Thus, the distribution ratio is calculated as the ratio of organic and aqueous phase concentrations of neodymium, according to Equation 2-7:

$$\therefore D_{Nd} = \frac{[Nd]_{organic}}{[Nd]_{aqueous}} = \frac{1988.94}{186.33} = 10.974$$

D.4: Uncertainties

Uncertainties of Measurement

The standard uncertainties, $u_i (\theta)$, for each measurement device, as well as the ICP calibration uncertainty for each experimental run, is listed in Table D-8. A sample calculation for determining $u_i (\theta)$ for the analytical mass balance is presented. This is considered a Type B uncertainty. The method is based on that specified by NIST, and was applied to the remaining associated Type B uncertainties (NIST, 2019).

Table D-8: Combined Standard Uncertainties

Device	Brand	Uncertainty of Measurement	Average Measurement	Standard uncertainty[a], $u_i (\theta)$
Analytical mass balance	Ohaus, Adventurer	: ±0.0006g	18.663 g	1.856×10^{-5}
Pt100 sensor		: ±0.14°C	23.733 °C	0.00341
Micropipette	IsoLab(5mL)	±0.02 mL	5 mL	0.00231
Micropipette	IsoLab(1mL)	±0.02 mL	1 mL	0.0115
Titration apparatus	Metrohm Titrando (888)	Uncertainty: ±0.0001 mL	2.675 mL	2.158×10^{-5}
ICP-OES (Perkin Elmer Optima 8300) Nd Calibration: Run 1[b]				1.161
ICP-OES (Perkin Elmer Optima 8300) Fe Calibration: Run 2[c]				0.594
ICP-OES (Perkin Elmer Optima 8300) Fe Calibration: Run 4[d]				1.710
ICP-OES (Perkin Elmer Optima 8300) Nd Calibration: Run 4[e]				1.807

[a] Uncertainties reported for all measurement devices, except the ICP-OES instrument, are Type B uncertainties, that are assumed to be rectangular (NIST, 2019). ICP-OES contributions are Type A uncertainties, since the uncertainty due to calibration is considered (NIST, 2019).

[b] Nd calibration standards were prepared during the post-graduate study (Bayeni, 2021).

[c] Fe calibration standard prepared with 85% pure Iron (III) Oxide in HNO_3

[d] Fe calibration standard prepared using an Fe ICP calibration standard of 1000ppm (99% pure)

[e] Nd calibration standard prepared using an Nd ICP calibration standard of 1000ppm (99% pure)

The uncertainty of measurement was reported by the manufacturer as 0.0006g (Trilab Support Balance and Scale Service, 2021). An average of all recorded masses (Appendix C) was calculated and reported in Table D-8. Thus, the manufacturer uncertainty is divided by the average mass measurement from this investigation to yield a dimensional form. Hence the standard uncertainty for the analytical balance is determined.

$$\therefore u_i(\theta) = \frac{\frac{18.663}{0.0006}}{\sqrt{3}} = 1.856 \times 10^{-5}$$

Calibration Uncertainties

The ICP calibration uncertainties are considered Type A uncertainties, and were determined in the form of the root mean square error (RMSE) (NIST, 2019). A sample calculation for a single calibration standard (Nd 401.224) from the neodymium test system (run 1) is presented. The same procedure was applied to the remaining uncertainties.

$$RMSE = \sqrt{\frac{\sum(Error)^2}{N}} = \sqrt{\frac{(-1.719)^2+(-0.693)^2+0.97^2+1.28^2+1.363^2+(-1.155)^2+(-0.045)^2}{9}} = 1.147$$

This was repeated for all calibration standards prepared and analysed. Since 3 neodymium standards were calibrated, an average of the RMSE was obtained to determine the standard uncertainty due to calibration for neodymium (in runs 1 and 4, respectively).

$$\therefore u_i(\theta) = \frac{1.147+1.189+1.146}{3} = 1.161$$

The calibration uncertainties for all experimental runs are presented in Table D-8.

Combined Standard Uncertainty

Thus, the uncertainties are combined for each experimental run as follows (NIST, 2019):

$$u_i(\theta) = \pm\sqrt{\sum(u_i(\theta))^2}$$

$$= \pm\sqrt{(1.856 \times 10^{-5})^2 + 0.00341^2 + 0.00231^2 + 0.0115^2 + (2.158 \times 10^{-5})^2 + (1.161)^2}$$

$$= 1.161$$

✓